

Nanomaterials for biology and medicine

Αντιγόνη Αλεξάνδρου

Antigoni Alexandrou

antigoni.alexandrou@polytechnique.edu

Laboratoire d'Optique et Biosciences, *Nanoimaging and cell dynamics team*

Ecole Polytechnique, CNRS, INSERM, Université Paris-Saclay

91128 Palaiseau Cedex, France



Nanomaterials for biology and medicine

Outline

- Nano-objects for bioapplications (quantum dots, lanthanide nanoparticles, metallic nanoparticles, carbon nanotubes, polymeric nanoparticles, ...): properties, characterization, advantages/disadvantages

- Short introduction to biology

- Biological applications: single-molecule imaging in cells, sensing of cell parameters (Ca^{2+} , ROS, pH)

- Biomedical applications (*in vitro* diagnostics, peroperative imaging, drug delivery, nanoparticle-sensitized radiation therapy)

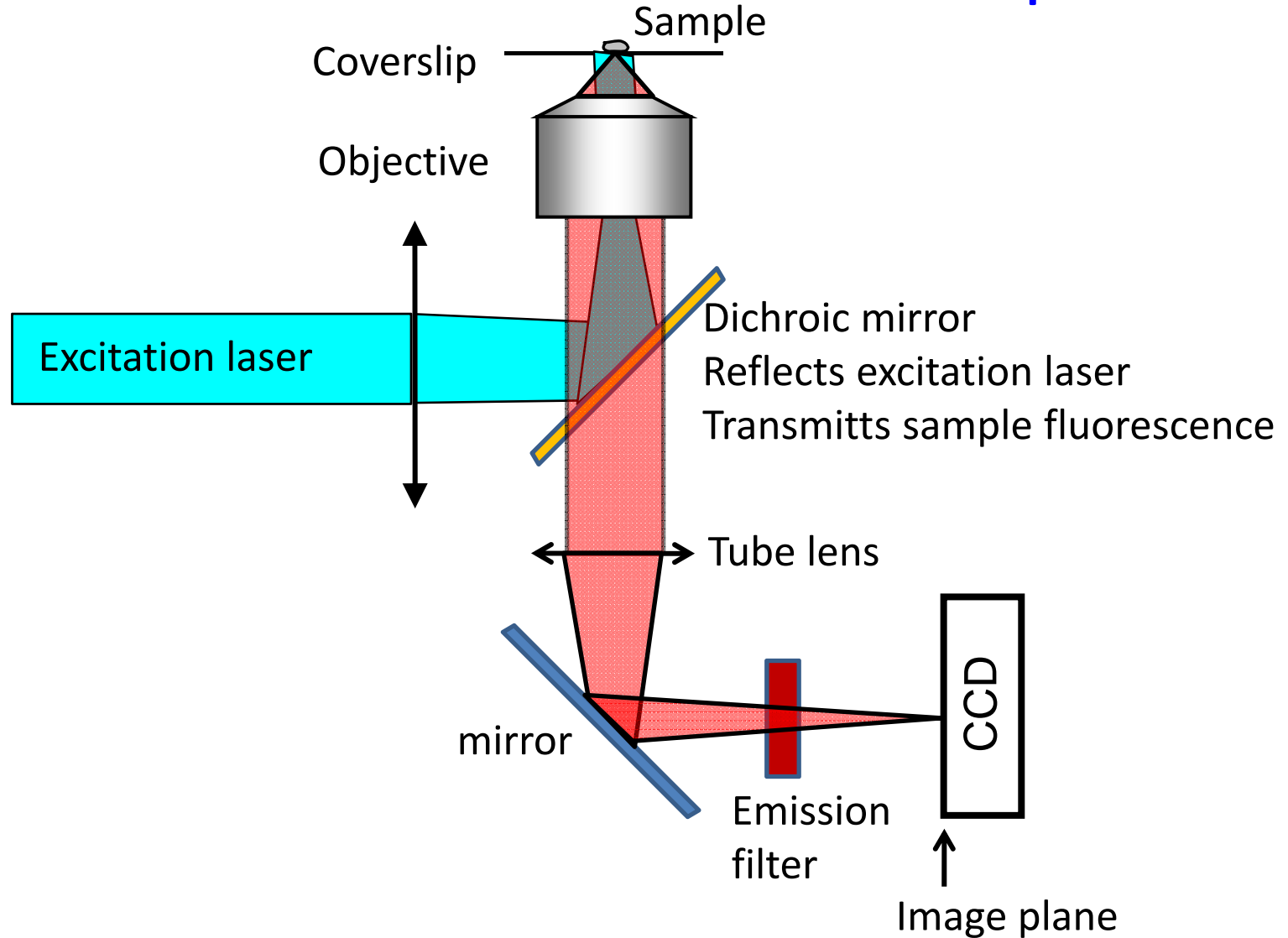
Nanoparticle applications for biology and medicine

- **Nanoparticles to observe and understand cell dynamics**
 - Nanoparticles for biomolecule labeling and tracking
 - Visualizing gene expression

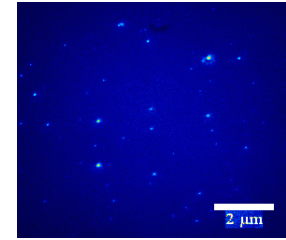
 - Nanoparticles for sensing
- ***In vitro* diagnostics**
- ***In vivo* applications**
 - Peroperative imaging
 - Drug delivery

Nanoparticles to observe and understand cell dynamics
Nanoparticles for single molecule tracking

Fluorescence imaging with a Wide-field inverted fluorescence microscope



Single molecule detection



Optical (lateral) resolution
(limited by diffraction):

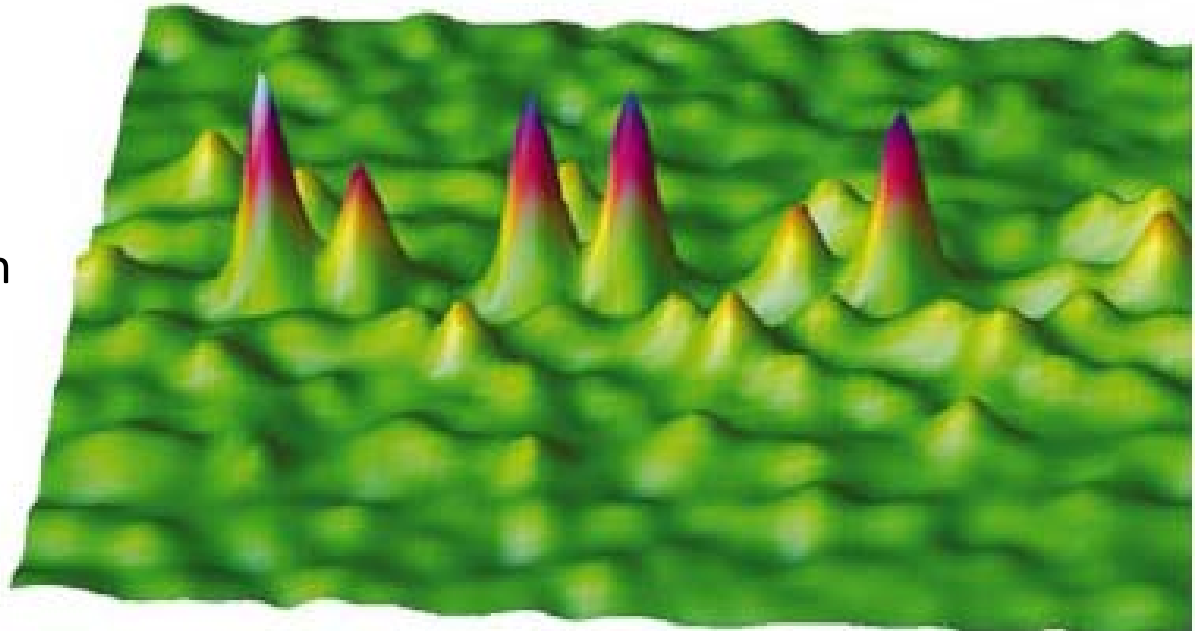
$$\Delta R = 1.22 \frac{\lambda}{2 N.A.} \quad N.A. = n \sin \theta$$

Typically : 200-300 nm

For single fluorescent objects

- the Airy disk can be fitted with a 2D Gaussian
- the center of the diffraction-limited spot can be determined from the Gaussian fit with a precision depending on the signal/noise ratio

**-> localization precision
down to 1 nm!**

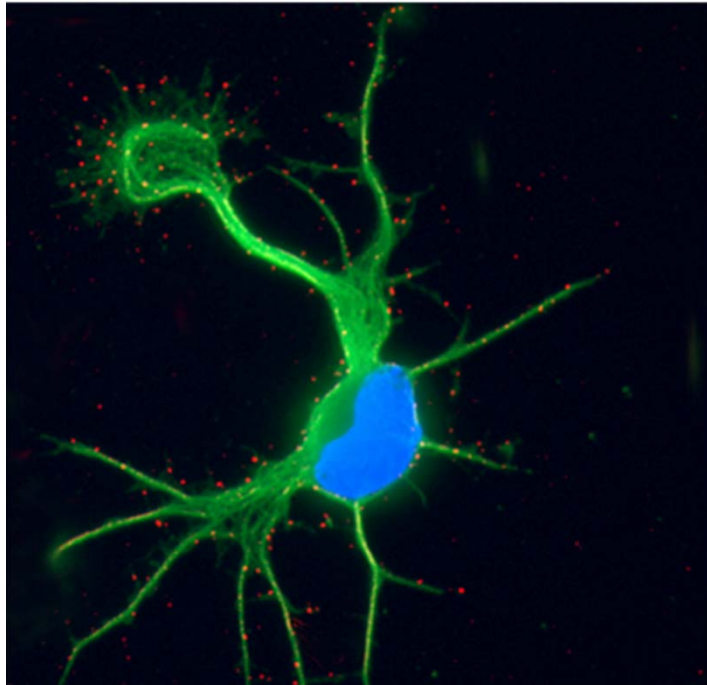


W. E. Moerner and D. P. Fromm,
Rev. Sci. Instrum. **74**, 3597 (2003).

Diffusion of GABA receptors in nerve growth cones revealed by single-QD tracking

Alternating directed and Brownian motion

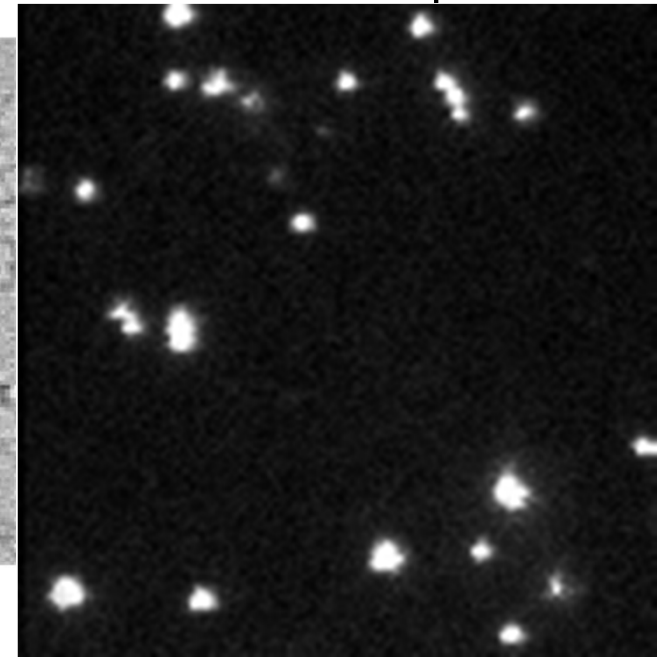
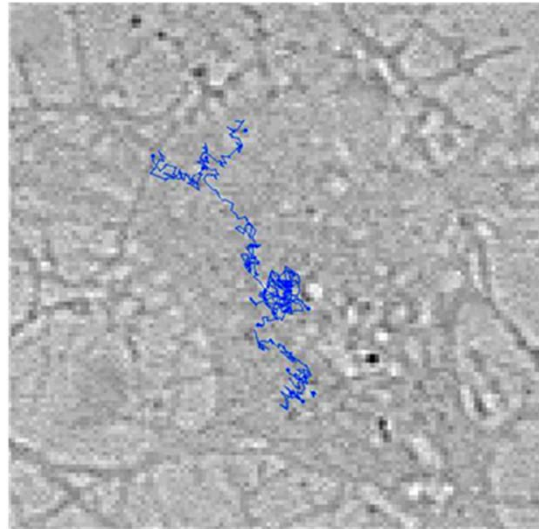
Imaging of QDs labeling
GABA receptors



C. Bouzigues

Red: QDs
Green: Microtubules
Blue: Nucleus

White-light transmission

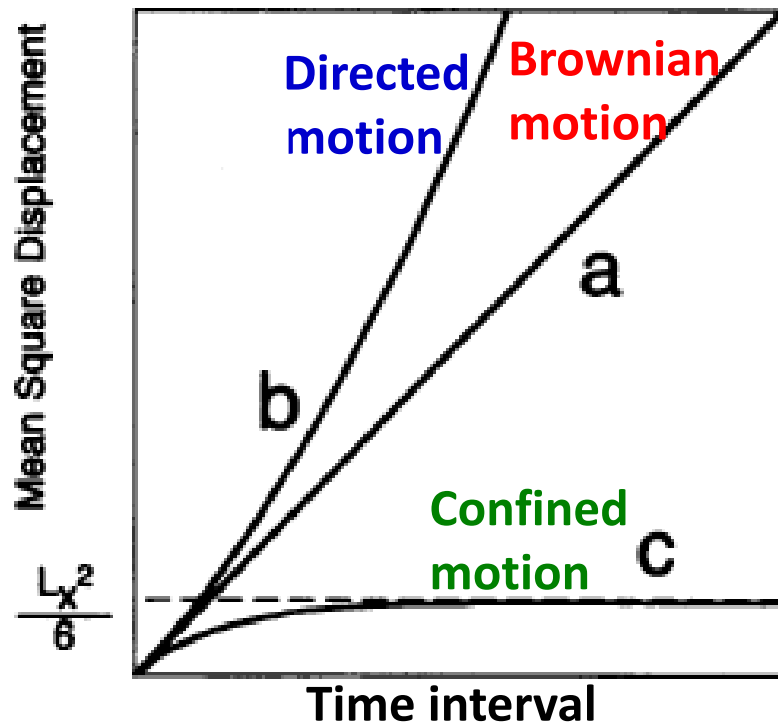


Use a **speed correlation index** to determine the portions of the trajectory corresponding to directed motion.

C. Bouzigues & M. Dahan, Biophys. J. 92, 654 (2007)

C. Bouzigues et al., Proc. Natl. Acad. Sci USA 104, 11251 (2007)

Analysis using the mean square displacement (MSD)



Case a: free Brownian diffusion

$$\begin{aligned} \text{MSD}_x(\Delta t) &= 2D_x \Delta t, \\ \text{MSD}_y(\Delta t) &= 2D_y \Delta t \\ \text{MSD}(\Delta t) &= 4D \Delta t \end{aligned}$$

$$4D = 2D_x + 2D_y$$

Case a: directed diffusion with a constant drift velocity v

$$\text{MSD}(\Delta t) = 4D\Delta t + v^2(\Delta t)^2$$

Case c: free Brownian diffusion inside an infinitely high square well potential

$$\langle x^2 \rangle(t) = \frac{L_x^2}{6} - \frac{16L_x^2}{\pi^4} \sum_{n=1(\text{odd})}^{\infty} \frac{1}{n^4} \exp\left\{ -\frac{1}{2} \left(\frac{n\pi\sigma_x}{L_x} \right)^2 t \right\}$$

$$\langle y^2 \rangle(t) = \frac{L_y^2}{6} - \frac{16L_y^2}{\pi^4} \sum_{n=1(\text{odd})}^{\infty} \frac{1}{n^4} \exp\left\{ -\frac{1}{2} \left(\frac{n\pi\sigma_y}{L_y} \right)^2 t \right\}$$

$$\sigma_x^2 = 2D_x, \quad \sigma_y^2 = 2D_y, \quad 4D = 2D_x + 2D_y$$

$$L_r^2 = L_x^2 + L_y^2.$$

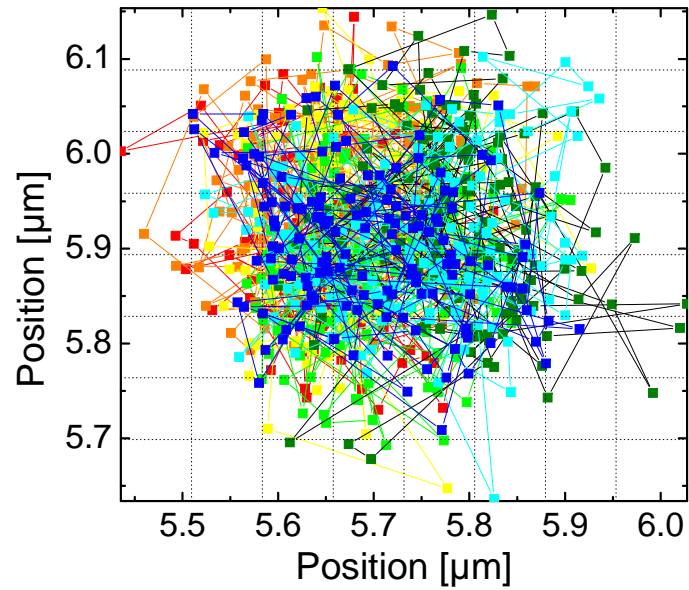
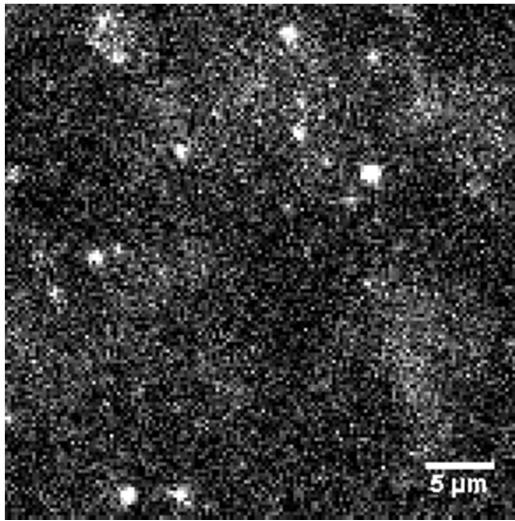
In all cases, the initial slope gives the diffusion coefficient D .

A. Kusumi et al, Biophys. J. 65, 2021 (1993).

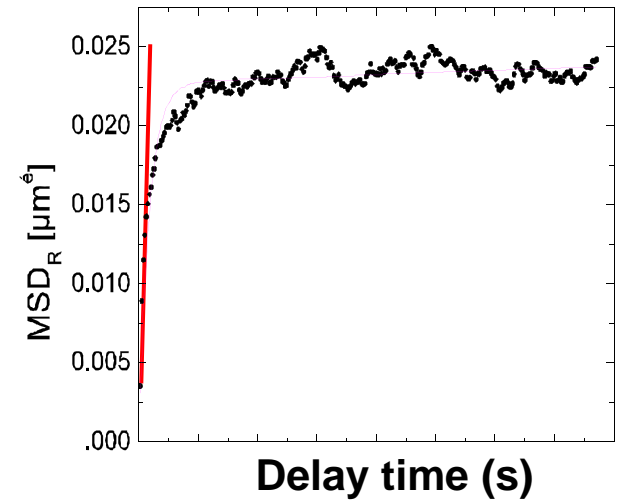
M. J. Saxton, K. Jacobson, Annu. Rev. Biophys. Biomol. Struct. 26, 373 (1997).

Single biomolecule tracking

Tracking proteins diffusing in the membrane



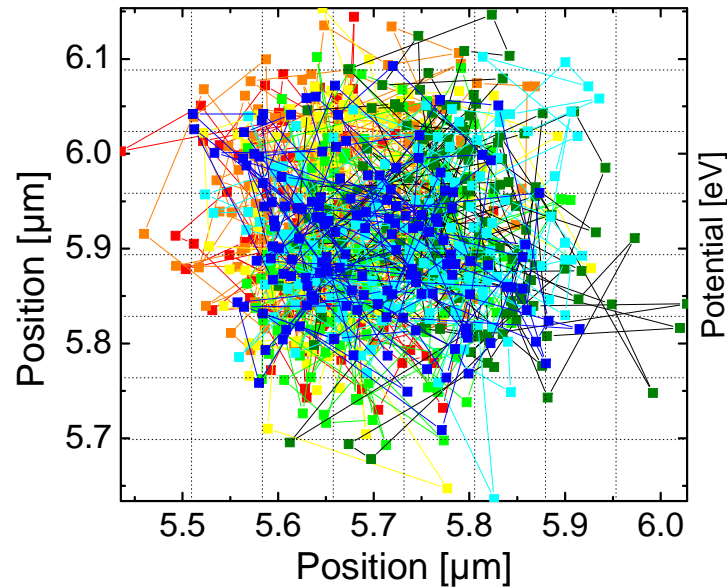
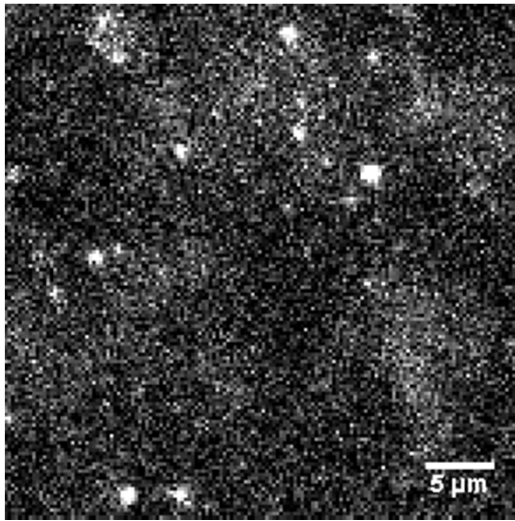
Standard analysis: mean square displacement



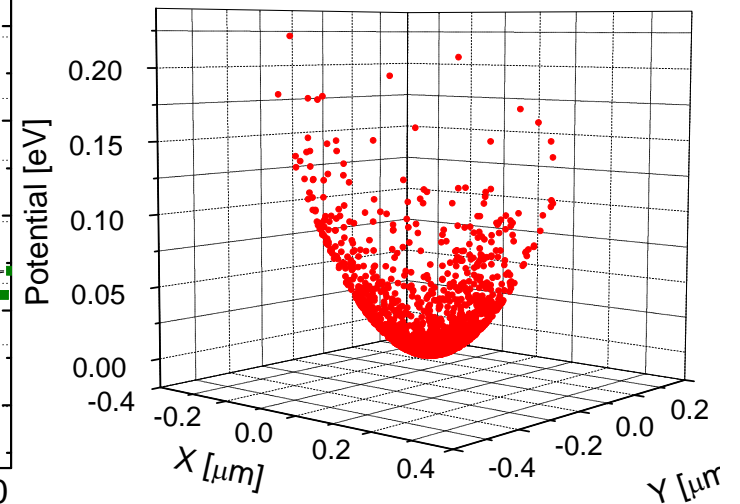
-> Diffusion coefficient D

Single biomolecule tracking

Tracking proteins diffusing in the membrane



Novel analysis based
on Bayesian inference



Extract
Potential felt by the receptor
in addition to the diff. coeff.

J.-B. Masson, ..., AA, PRL 2009; G. Voisinne, AA, Masson, Biophys. J. 2010

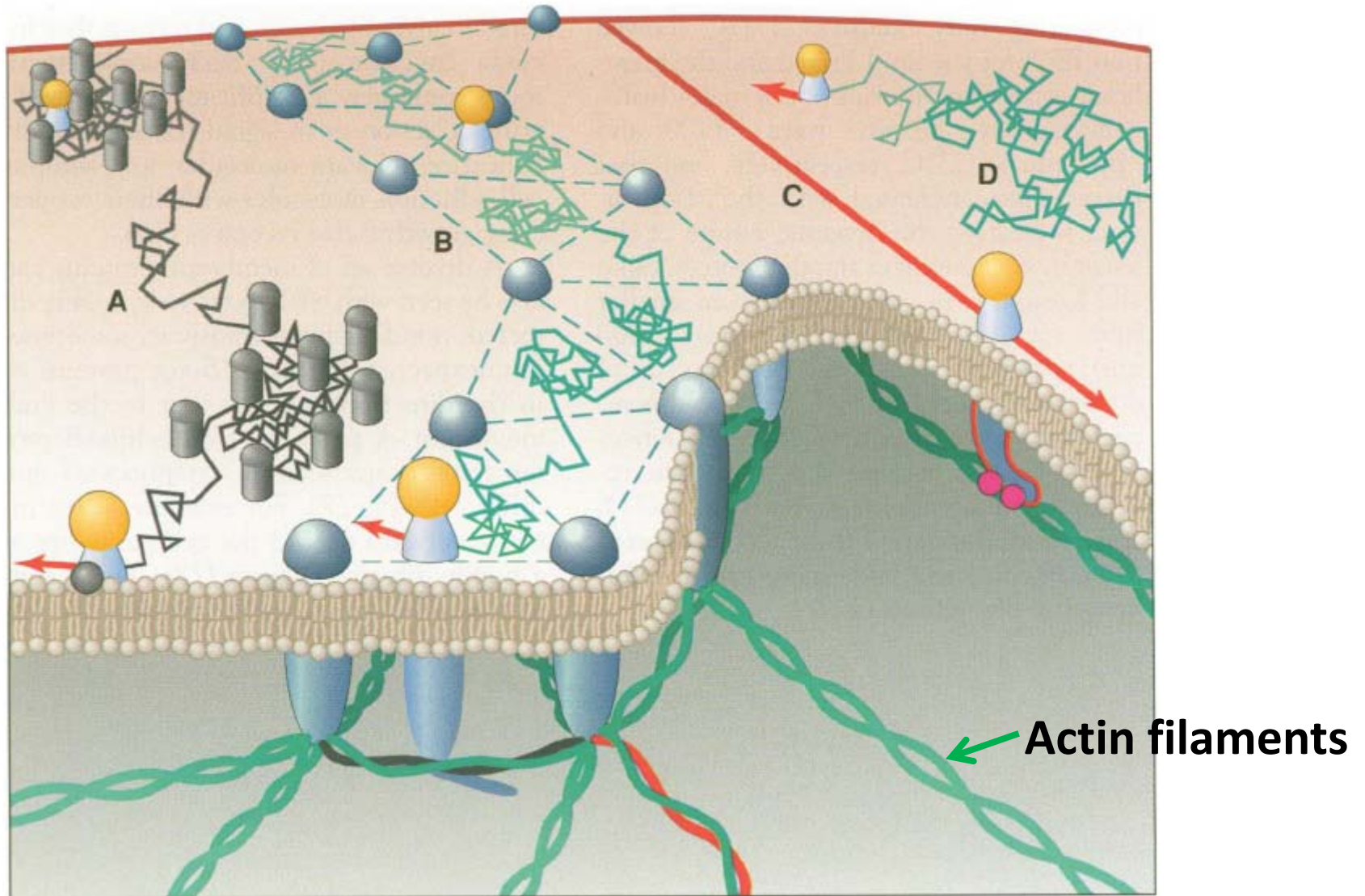
S. Türkcan, AA, Masson, Biophys. J. 2012

S. Türkcan, ..., Masson, AA, Biophys. J. 2012

Collaboration with J.-B. Masson and M. R. Popoff, Institut Pasteur, Paris

Different types of membrane compartmentation

Cytoskeleton microdomains

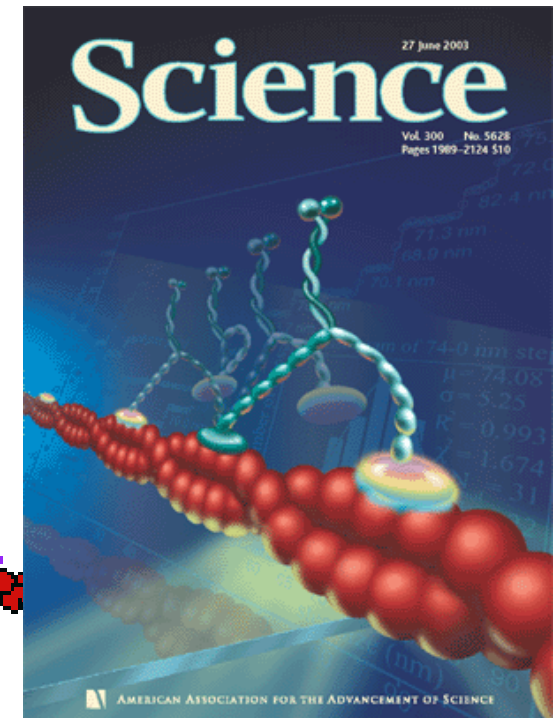
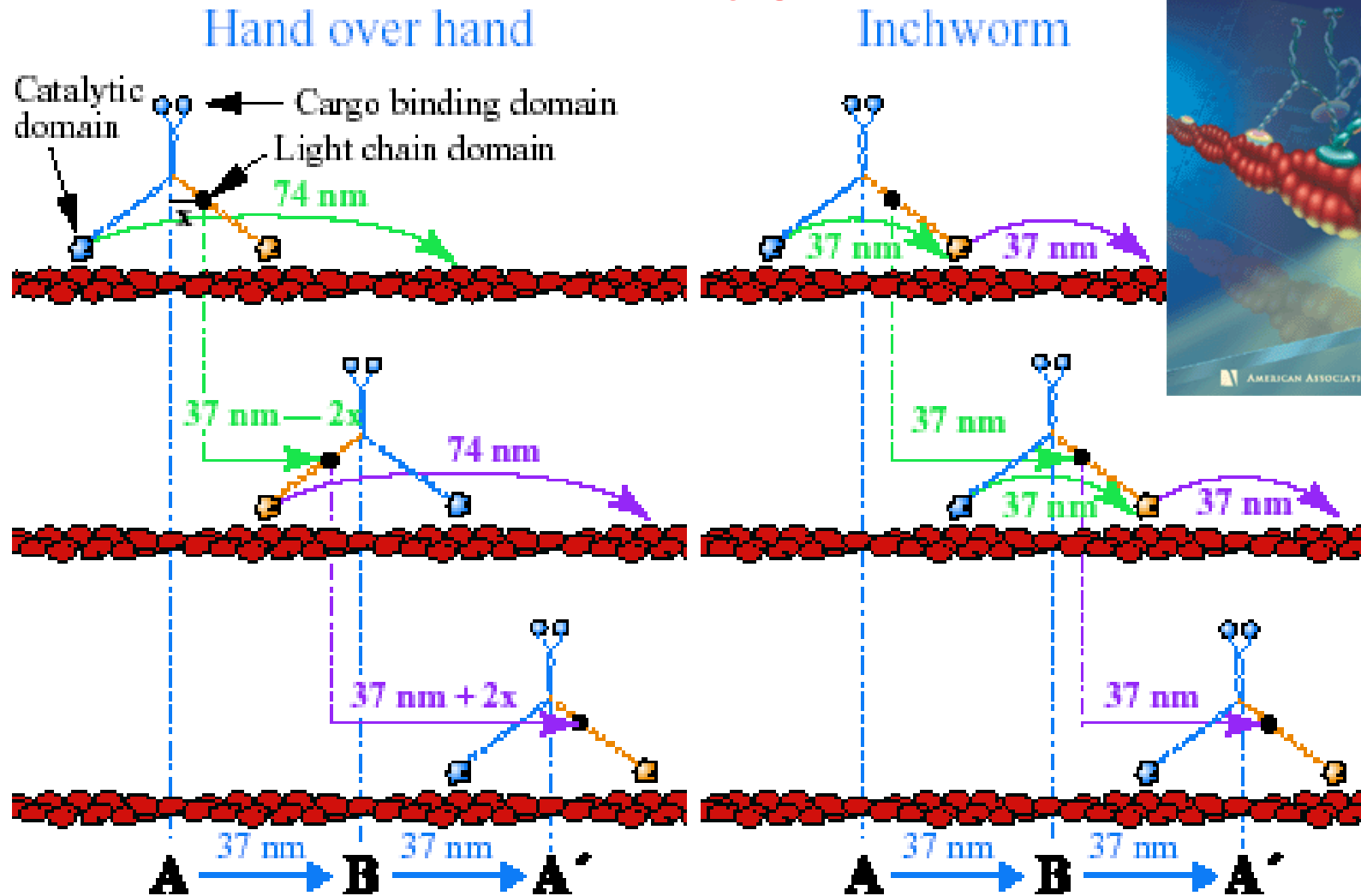


K. Jacobson, E. Sheets & R. Simson, Science 268, 1441 (1995)

Single biomolecule tracking

Myosin V motion on actin filaments

In vitro

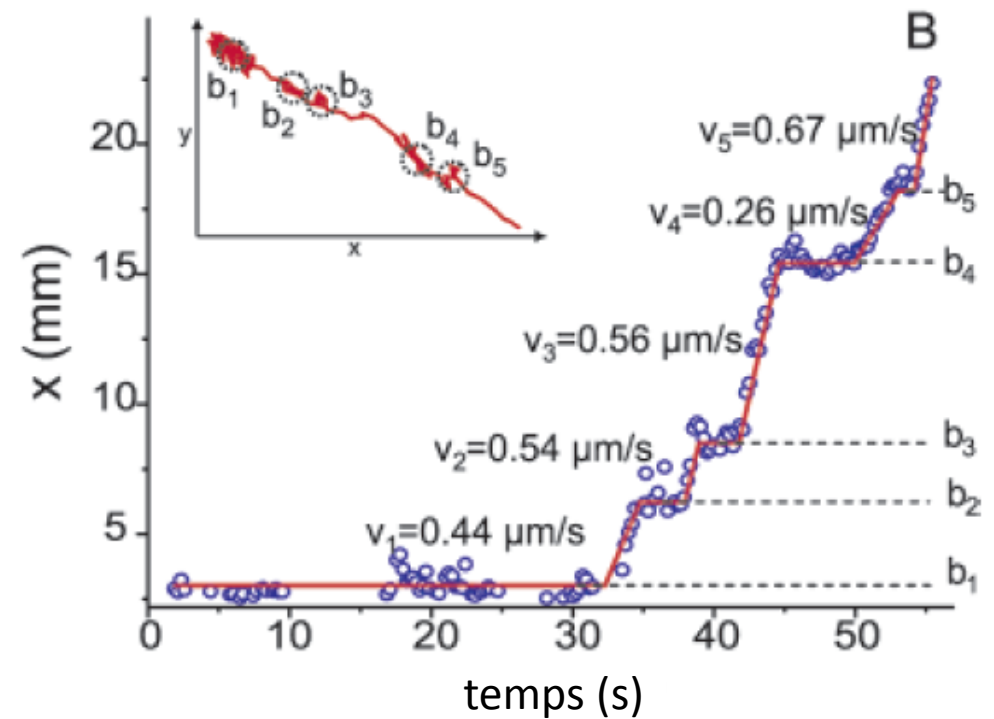
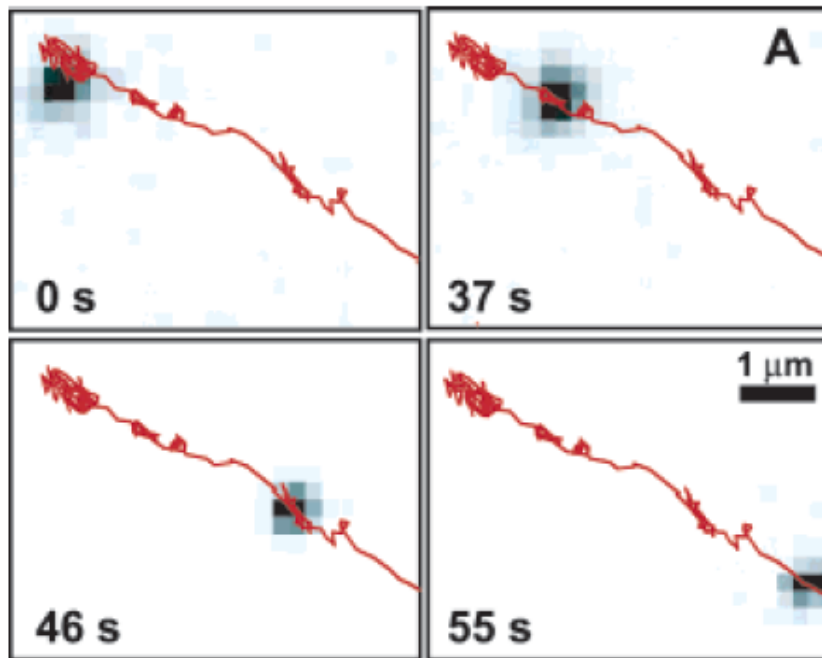


P. Selvin's group, University of Illinois
Yildiz et al., Science **300**, 2061 (2003).

Single biomolecule tracking

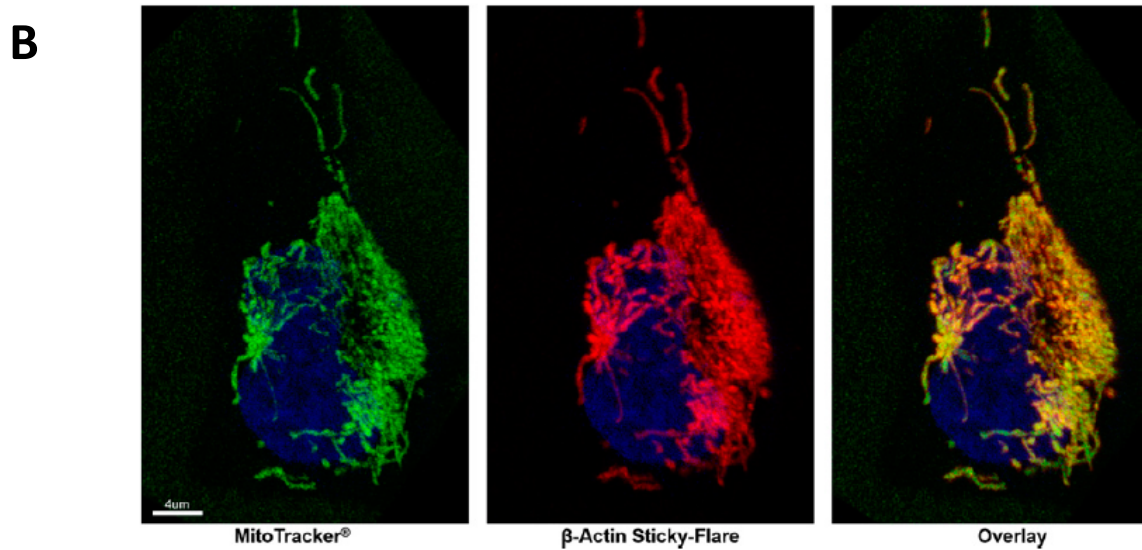
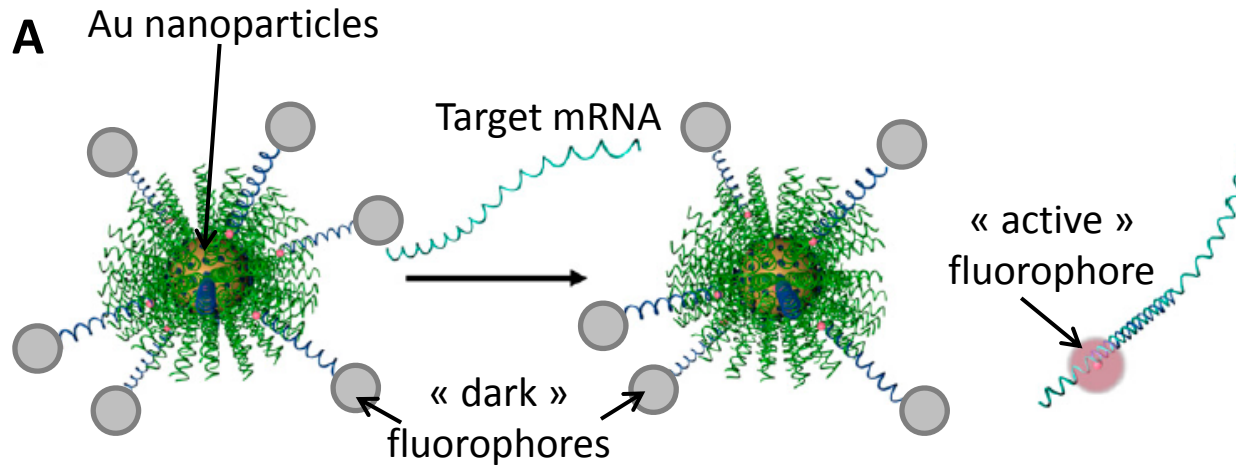
Tracking proteins diffusing inside the cell

Kinesin « walking » on microtubules



Imaging and tracking mRNA with « sticky flares »

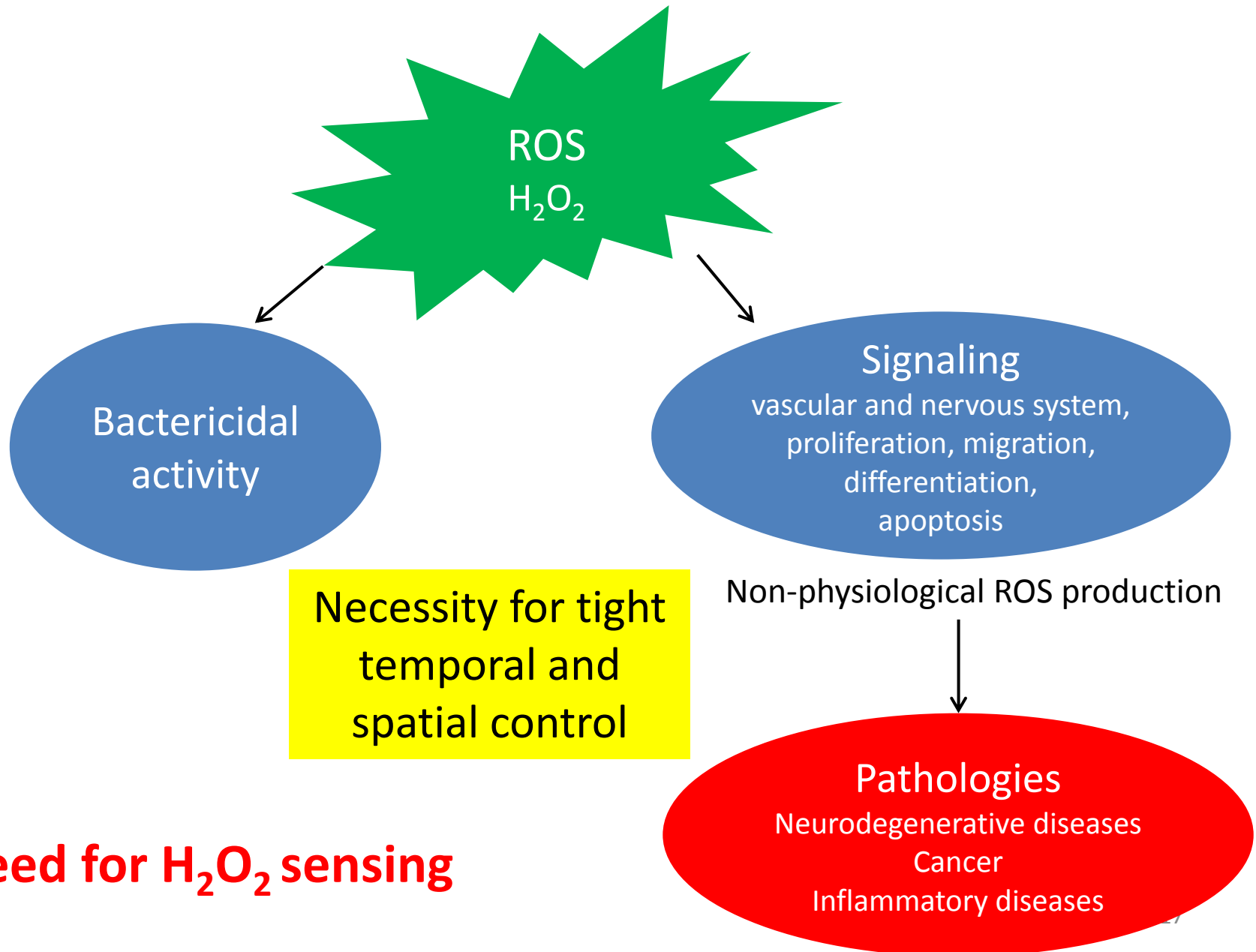
Quenching of organic fluorophores by Au nanoparticles



Briley et al, Proc. Natl. Acad. Sci. USA 112, 9591 (2015)

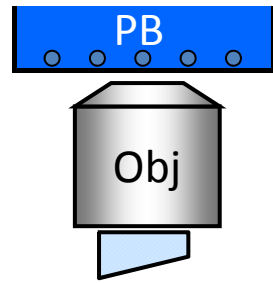
Nanoparticles to observe and understand cell dynamics
Nanoparticles for sensing intracellular parameters

Reactive oxygen species (ROS)



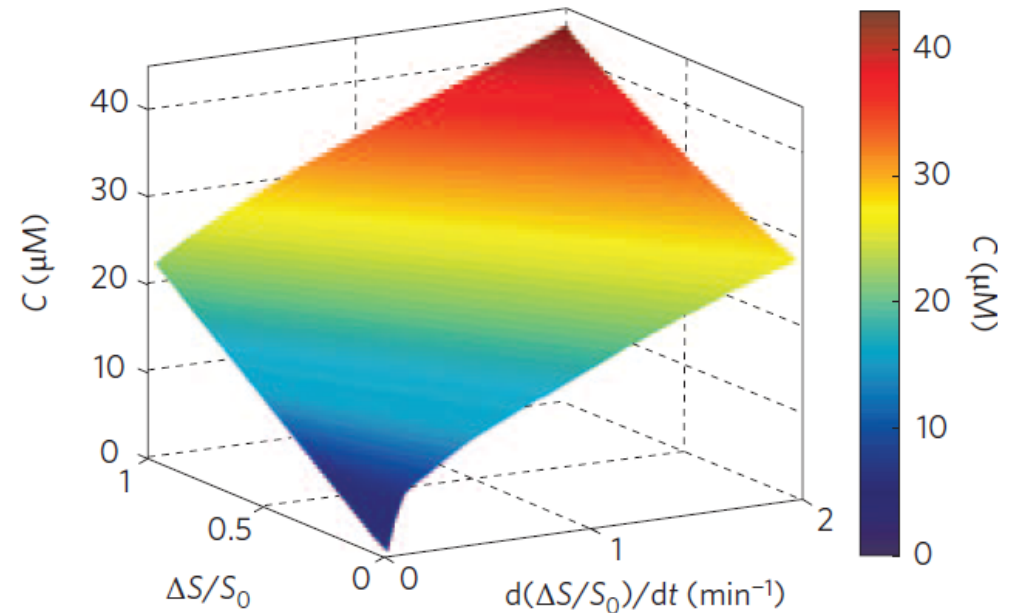
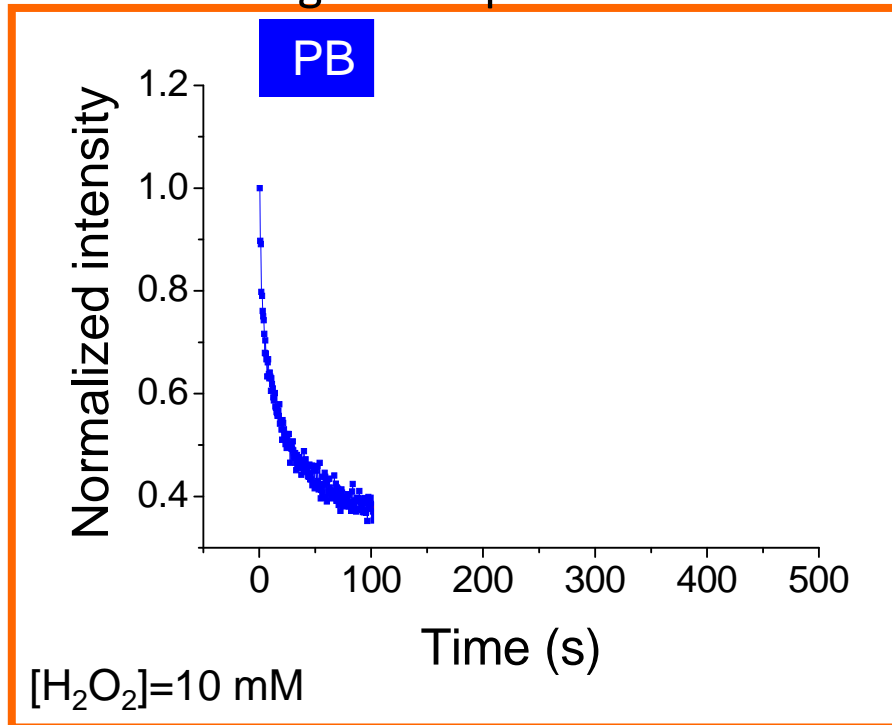
-> Need for H₂O₂ sensing

Spincoated NPs



$Y_{0.6}Eu_{0.4}VO_4$ Nanoparticles for H_2O_2 sensing

Single nanoparticle



acquisition time: 500 ms laser intensity: 5-6 kW/cm²

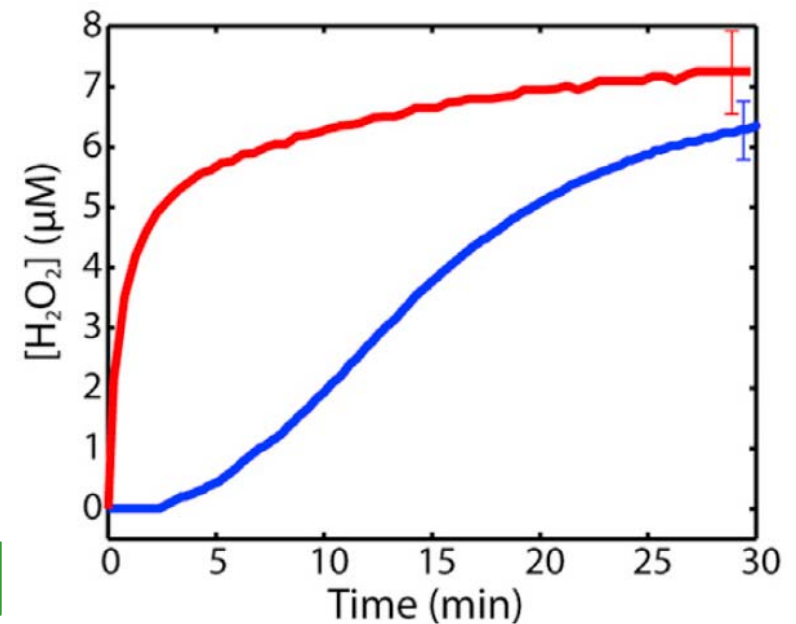
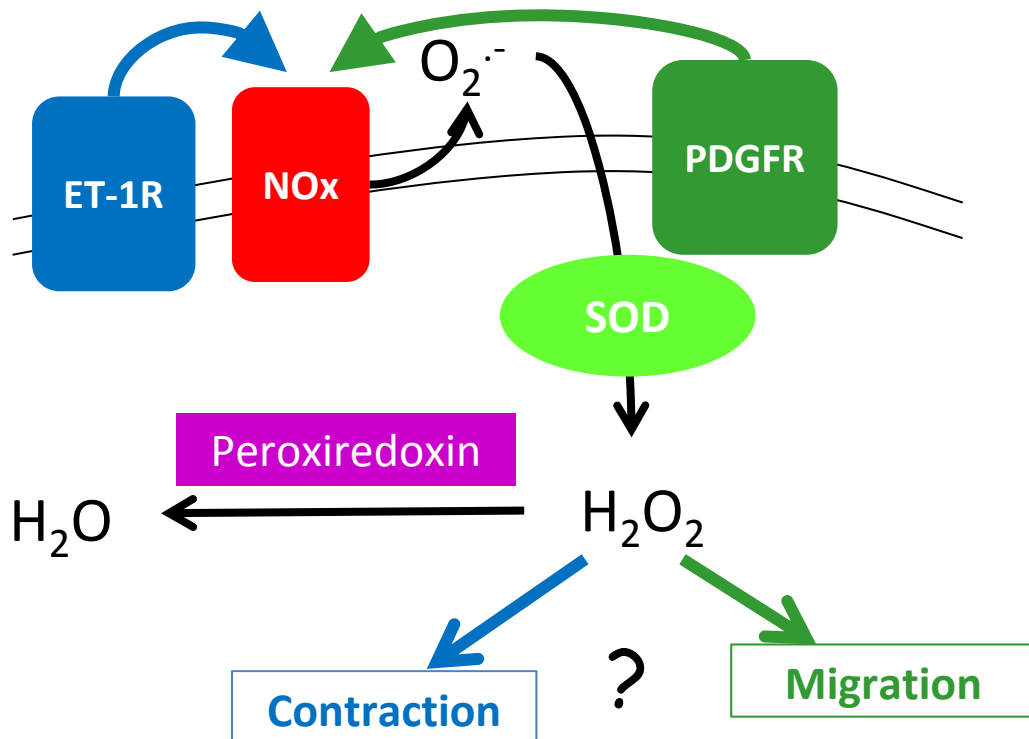
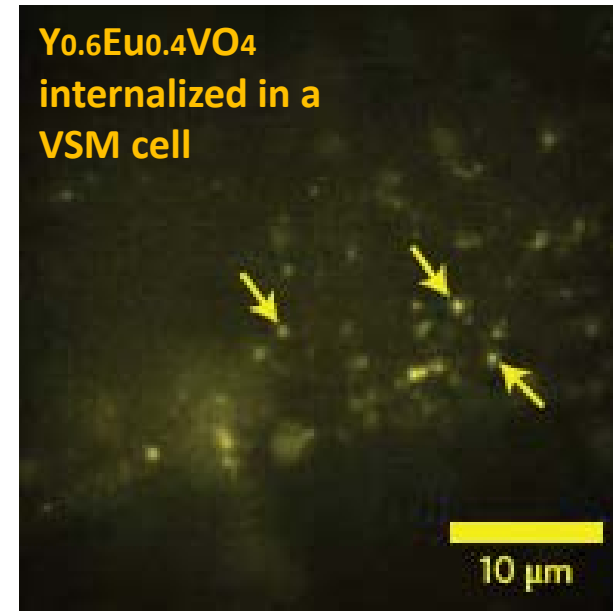
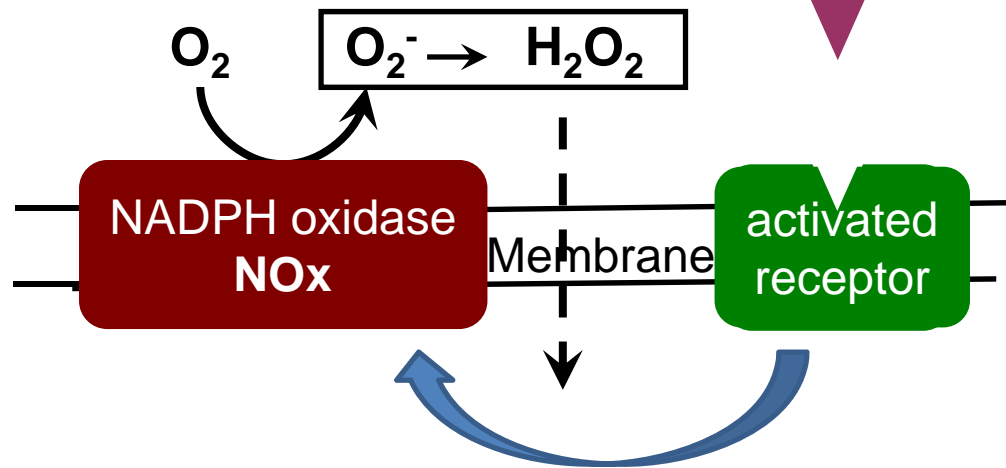
-> Laser-induced Eu^{3+} reduction



-> H_2O_2 -induced Eu^{2+} oxidation



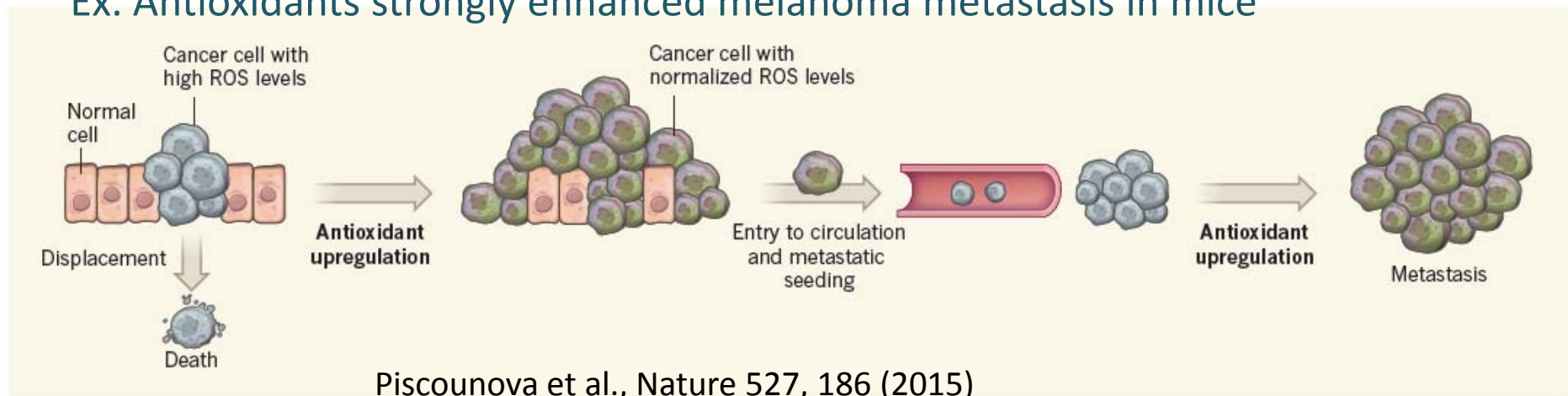
Nanoparticles for H₂O₂ sensing during cell signaling



ROS and Cancer: a complex interaction

- **Chronic inflammation <-> Cancer** (*helicobacter pilori*->gastric ulcer->gastric cancer)
Barry Marshall & Robin Warren, Nobel prize 2005
Crusz, S. M. & Balkwill, F. R. *Nat. Rev. Clin. Oncol.* 12, 584–596 (2015)
-> **Anti-inflammatory approaches to treat cancer**
- ROS oxidative stress -> enhanced mutation rates -> cancer cells
- ROS driving tumor initiation and progression
-> **Anti-oxidant approaches to treat cancer -> Opposite results obtained**
- **ROS: Dual ability to promote or suppress tumor development in different contexts**

Ex. Antioxidants strongly enhanced melanoma metastasis in mice

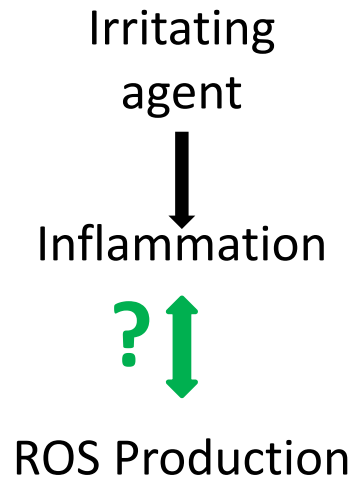


Piscounova et al., *Nature* 527, 186 (2015)

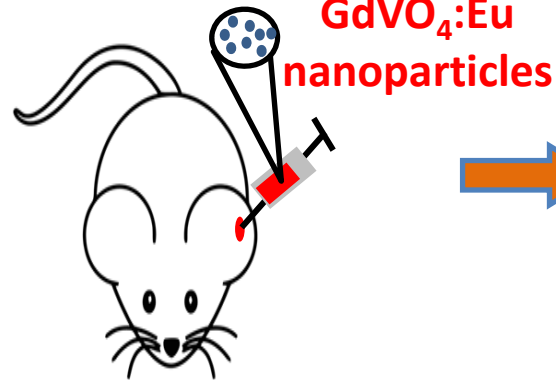
Harris, Brugge, *Nature (News & Views)* 527, 170 (2015)

Sensing ROS with Eu-doped nanoparticles *in vivo*

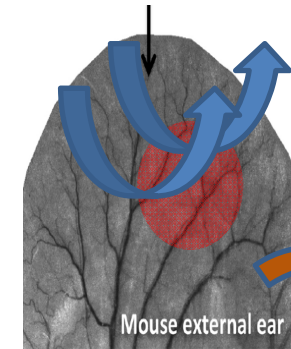
in vivo inflammation model



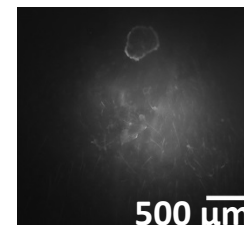
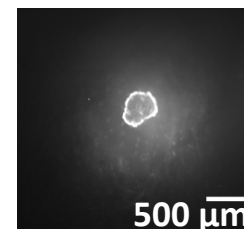
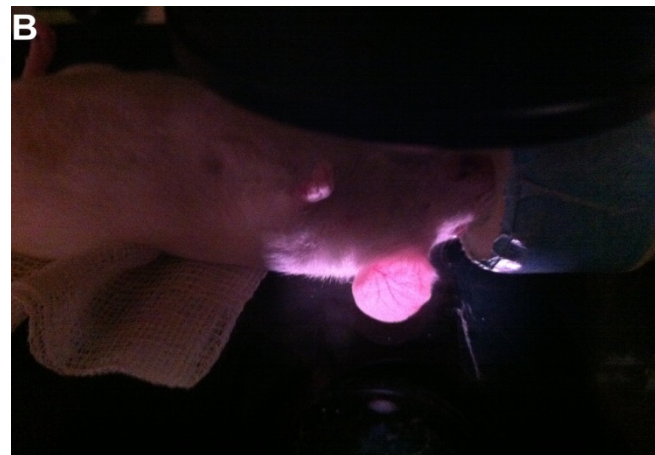
Inflammation model
in mouse



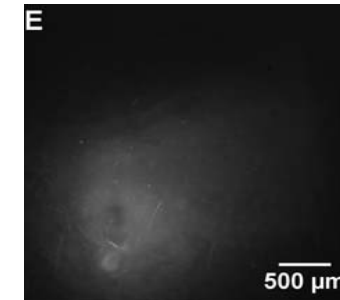
Topical application of
methylsalicylate



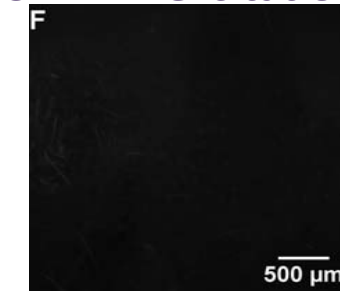
Kalchenko *et al.* J. Biomed. Opt. (2014)



466 nm excitation

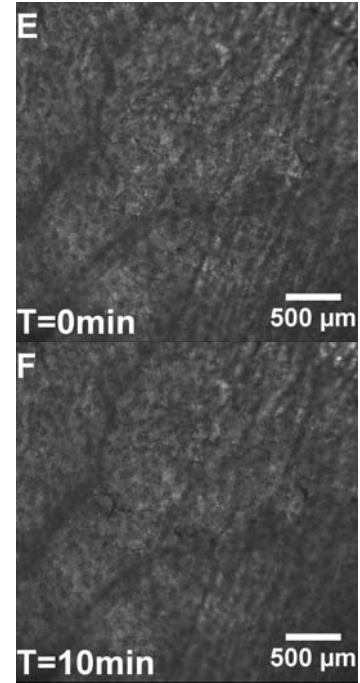
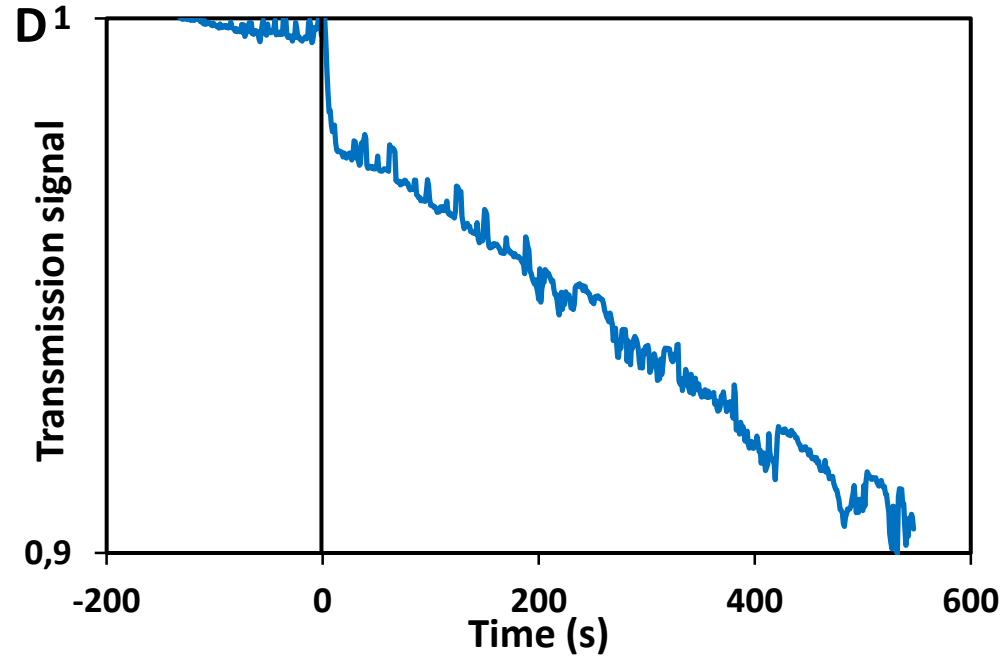


377 nm excitation

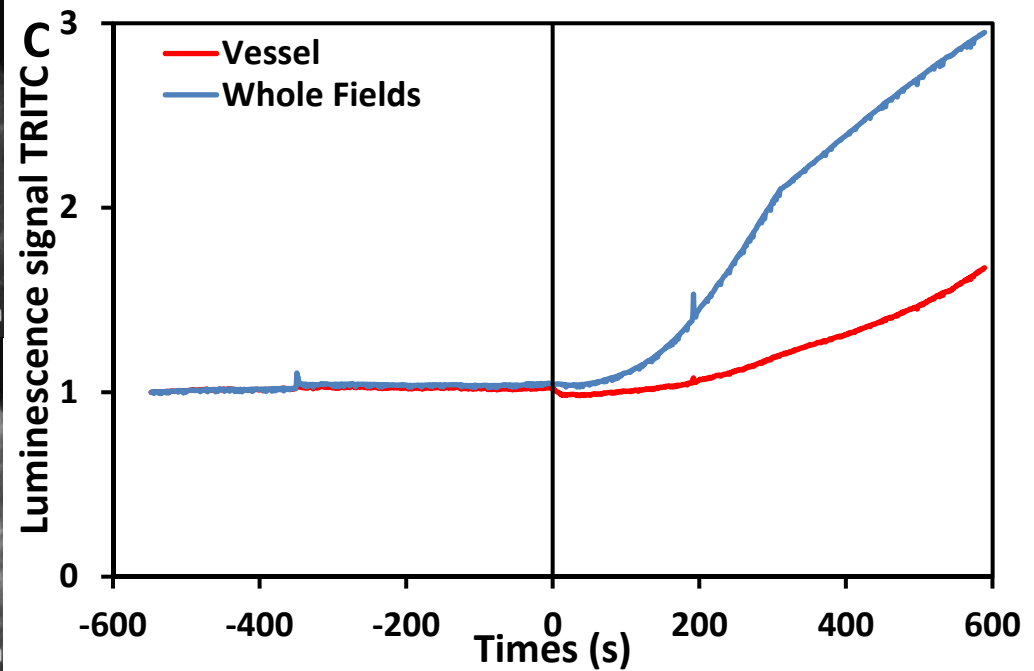
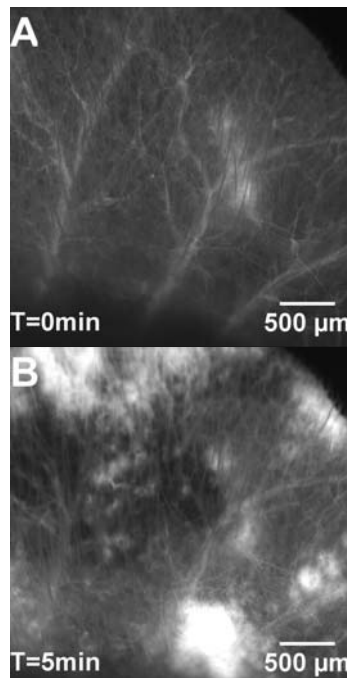


Mouse ear inflammation model

Transmitted
signal

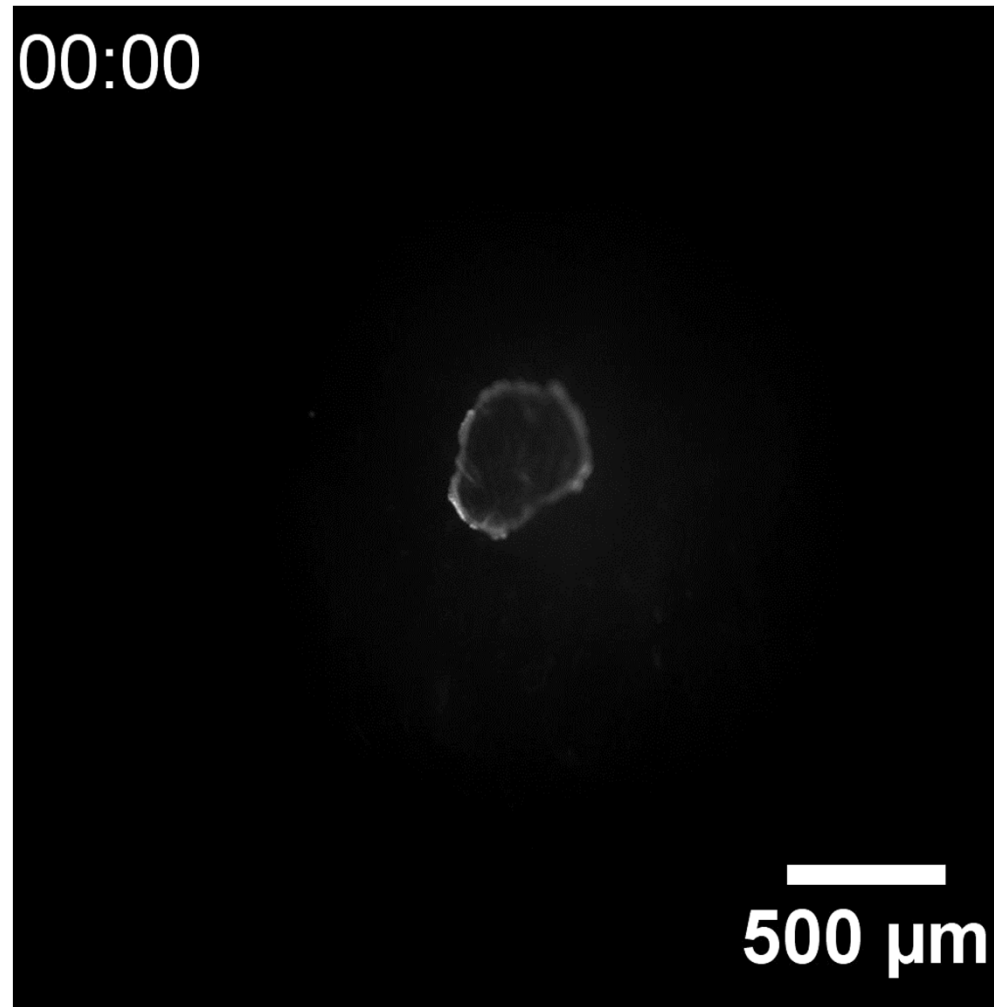


Dextran TRITC
angiography

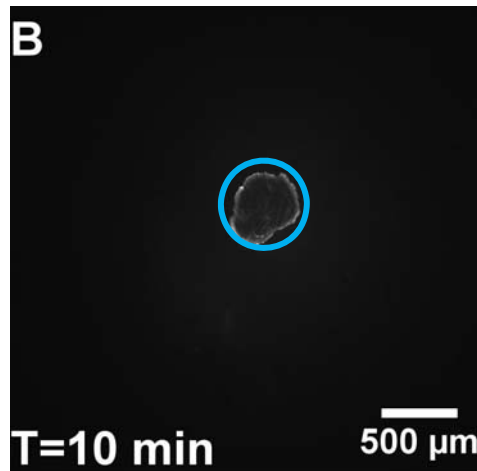
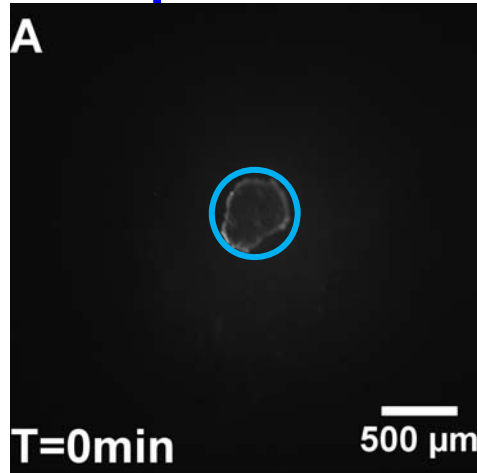


ROS production *in vivo*

Flash at 2 min :
methylsalicylate
application
At 7:30 min :
luminescence
recovery

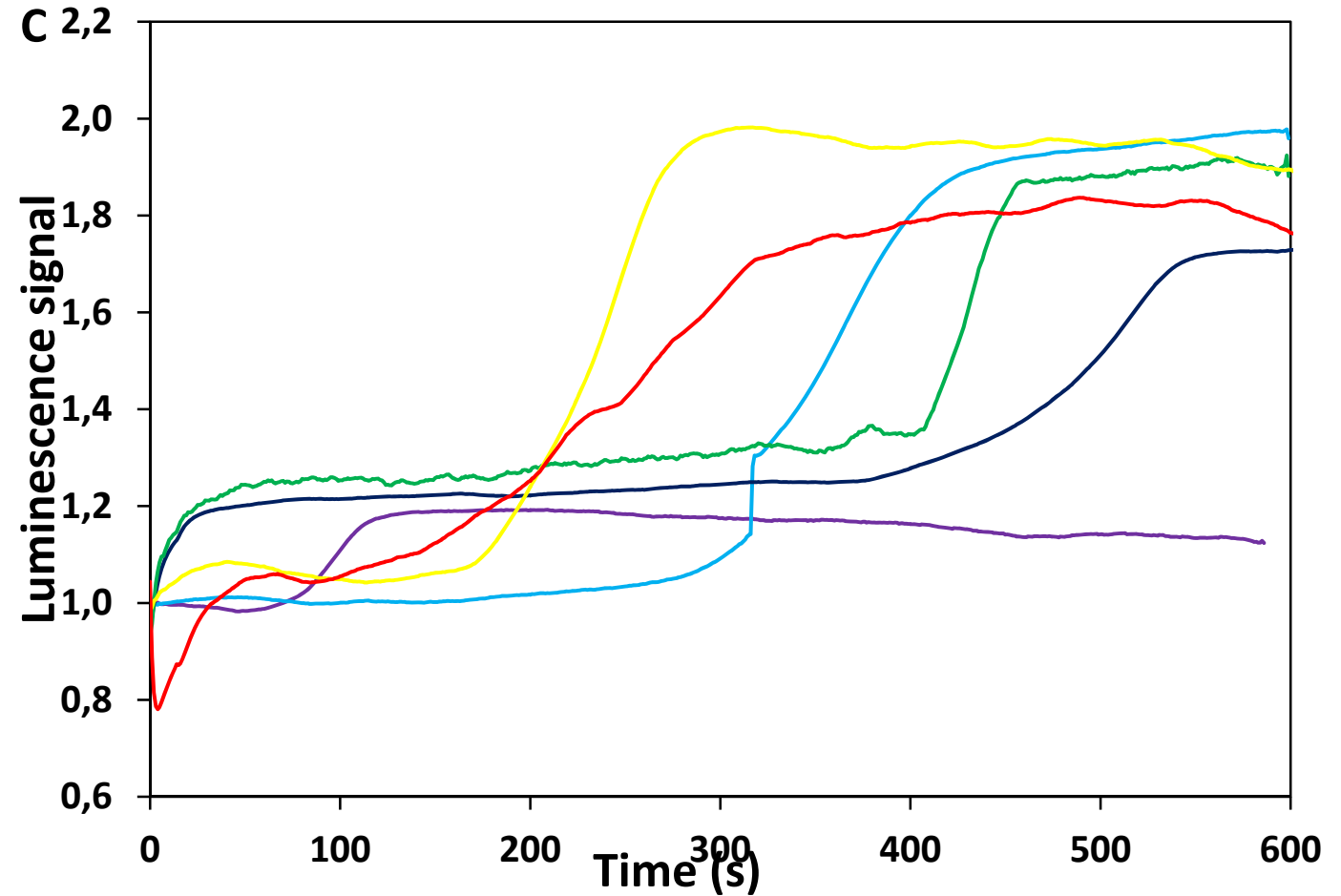


Sensing ROS with Eu-doped nanoparticles



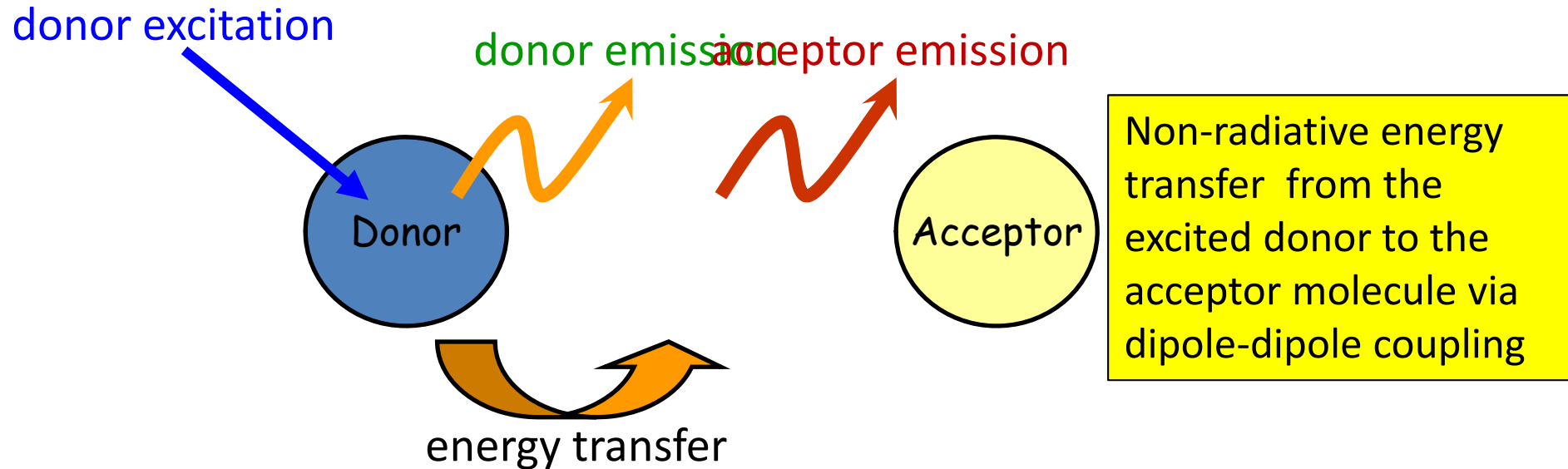
Measuring ROS production *in vivo*

t=0
Methylsalicylate
application



**Luminescence recovery in mouse ear experiments (N=6)
=> *in vivo* ROS detection**

Förster resonant energy transfer (FRET)



In the presence of resonant energy transfer:

- decrease of donor emission
- increase of acceptor emission
- decrease of donor lifetime

Energy transfer depends on the 6th power of donor-acceptor distance

-> spectroscopic ruler

Prerequisites:

- Overlap between donor emission and acceptor absorption spectra
- Extensively used in biology to observe distance changes (2-10 nm):

- Interaction between biomolecules

- Conformational changes

T. Förster, *Annalen der Physik* 2, 55 (1948)

R. M. Clegg, *Curr. Op. Biotech.* 6, 103 (1995)

P. R. Selvin, *Methods in Enzymology*, Vol. 124, Academic Press (1995), p. 300

Förster resonant energy transfer (FRET)

Nonradiative induced dipole – induced dipole interaction

Point dipole approximation

A harmonically oscillating electric dipole p_D produces an electric field:

$$\rho = \rightarrow$$

$$\vec{E}_D(\vec{r}) = \frac{1}{4\pi\epsilon_0} \left[\frac{k^2}{r} (\vec{r}_0 \times \vec{p}_D) \times \vec{r}_0 + [3\vec{r}_0(\vec{r}_0 \cdot \vec{p}_D) - \vec{p}_D] \left(\frac{1}{r^3} - \frac{ik}{r^2} \right) \right] e^{ikr} \quad \vec{r} = \vec{r}_0 r$$

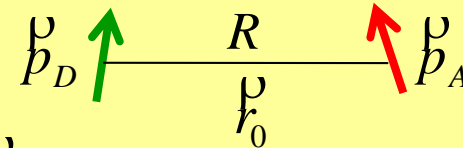
In the near field ($r \ll \lambda$):

$$\vec{E}_D = \frac{1}{4\pi\epsilon_0} \left[\frac{3\vec{r}_0(\vec{r}_0 \cdot \vec{p}_D) - \vec{p}_D}{r^3} \right] e^{ikr}$$

D: donor

A: acceptor

R: distance between the two dipoles



\vec{r}_0 : unit vector joining the two dipoles

Coupling with another point dipole p_A :

Interaction energy $V = -\vec{p}_A \cdot \vec{E}_D = -\frac{1}{4\pi\epsilon_0} \left[\frac{3(\vec{r}_0 \cdot \vec{p}_A)(\vec{r}_0 \cdot \vec{p}_D) - \vec{p}_A \cdot \vec{p}_D}{R^3} \right] e^{ikR}$

Fermi's golden rule gives the transition rate from the donor excited state to the acceptor excited state:

$$k_T = \frac{2\pi}{\eta} |\langle i | V | f \rangle|^2 \rho_f \propto \left(\frac{1}{R} \right)^6$$

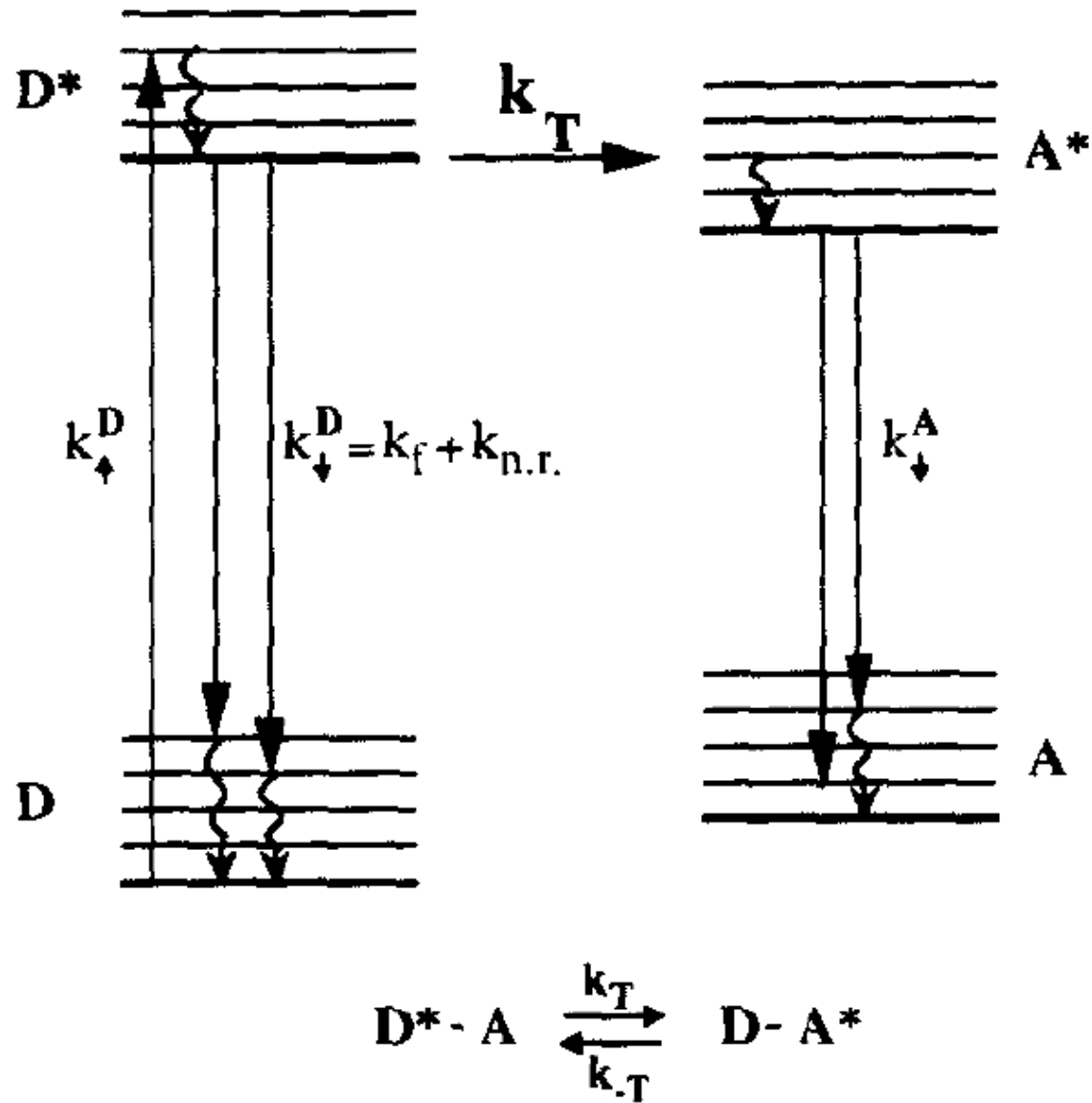
$|i\rangle = |D^* \rangle |A\rangle$ Initial state

$|f\rangle = |D\rangle |A^* \rangle$ Final state

ρ_f Density of final states

Förster resonant energy transfer (FRET)

Jablonski energy level diagram



Energy transfer rate and efficiency

$$E = \frac{k_T}{k_T + k_D}$$

$$k_T = k_D \left(\frac{R_0}{R} \right)^6$$

$$E = \frac{1}{1 + \left(\frac{R}{R_0} \right)^6}$$

E: efficiency of energy transfer (or FRET efficiency), defined as the **probability for the excited donor to return to its ground state by energy transfer to the acceptor**

k_T : rate of energy transfer to the acceptor

k_D : total rate of all other radiative and non-radiative donor decay processes $\tau_D = \frac{1}{k_D}$

R_0 : the distance R for which the energy transfer rate is equal to the donor excited-state decay rate

$$R_0 = 0.21 (J q_D n^{-4} \kappa^2)^{1/6} \text{ (in Angstroms)}$$

$$J = \int \varepsilon_A(\lambda) f_D(\lambda) \lambda^4 d\lambda / \int f_D(\lambda) d\lambda \text{ in } \underline{M}^{-1} \text{ cm}^{-1} \text{ nm}^4$$

J: normalized spectral overlap of the donor emission (f_D) and acceptor absorption (ε_A) in units of $M^{-1} \text{ cm}^{-1}$

κ^2 : depends on relative dipole orientation

q_D : donor quantum yield, n: refraction index

T. Förster, *Annalen der Physik* 2, 55 (1948)

P. R. Selvin, *Annu. Rev. Biophys. Biomol. Struct.* 31, 275 (2002)

P. R. Selvin. *Methods in Enzymology*, Vol. 124, Academic Press (1995), p. 300

$R_0 \sim 5\text{-}7 \text{ nm}$

Distance measurements: $\sim 2\text{-}10 \text{ nm}$

Measurements of energy transfer efficiency

Rewording the FRET efficiency definition: E is the donor fraction de-excited via energy transfer to the acceptor

$$E = 1 - \frac{I_{D_A}}{I_D}$$

I_D : donor emission intensity in the absence of the acceptor
 I_{D_A} : donor emission intensity in the presence of the acceptor

Intensity measurements: beware of pitfalls

-> In ensemble measurements, intensities must be normalized for concentration.

$$E = 1 - \frac{\tau_{D_A}}{\tau_D}$$

τ_D : excited-state lifetime of the donor in the absence of the acceptor
 τ_{D_A} : excited-state lifetime of the donor in the presence of the acceptor

The lifetime approach is concentration independent.

Alternatively:

$$E = \frac{I_{A_D} / q_A}{I_{A_D} / q_A + I_{D_A} / q_D}$$

I_{A_D} : FRET-induced acceptor emission intensity
 $q_{D(A)}$: Donor (acceptor) quantum yield

Beware of direct acceptor excitation

FRET donor-acceptor pairs

A large variety of FRET pairs exists:

- Dye->dye (ex. Cy3-> Cy5)
- Fluorescent protein-> fluorescent protein
- Nanoparticle -> dye
-

Quantum dot -> dye

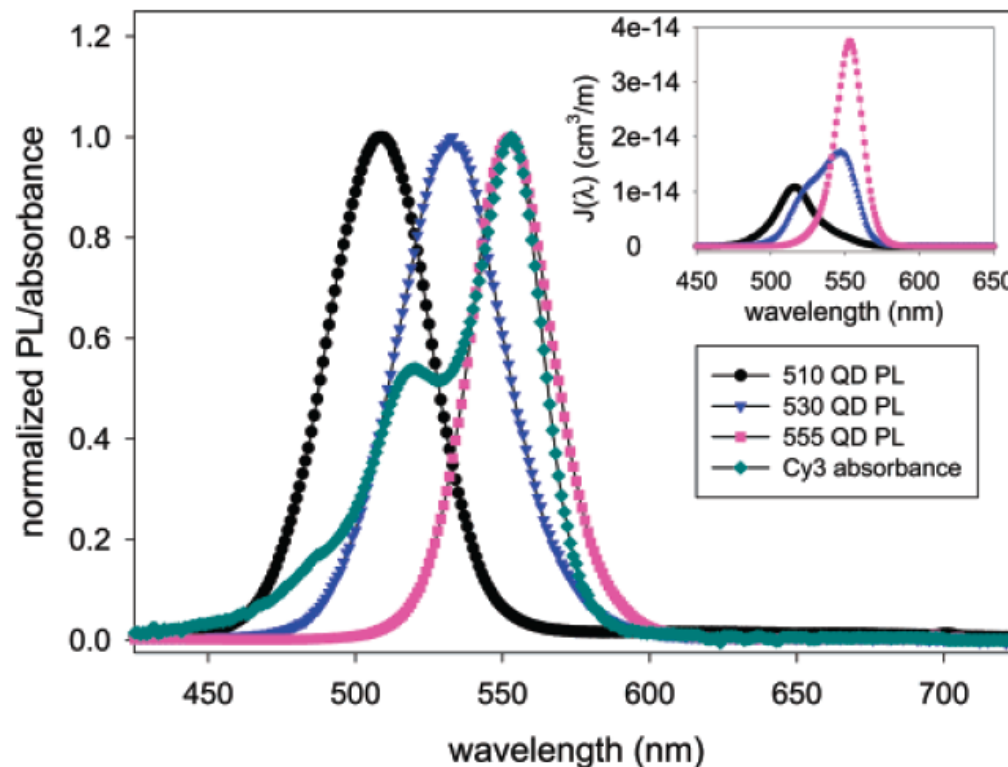
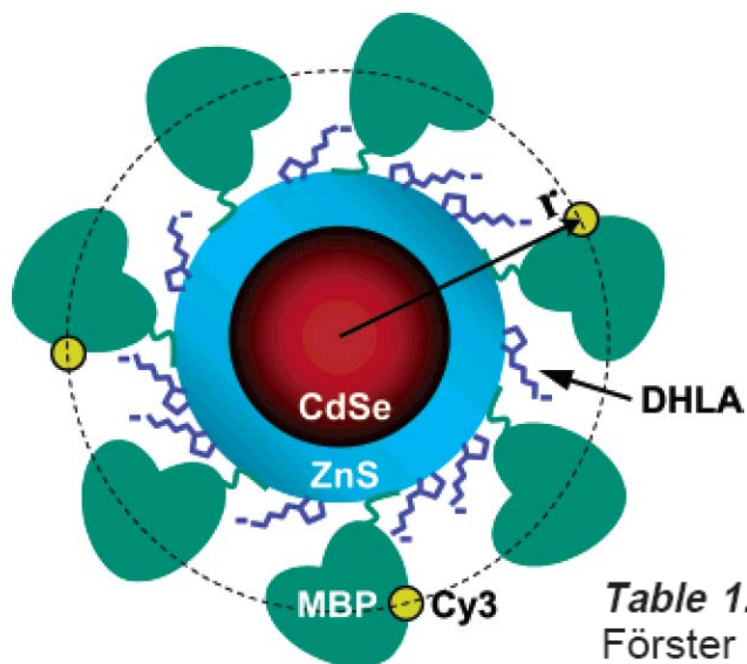


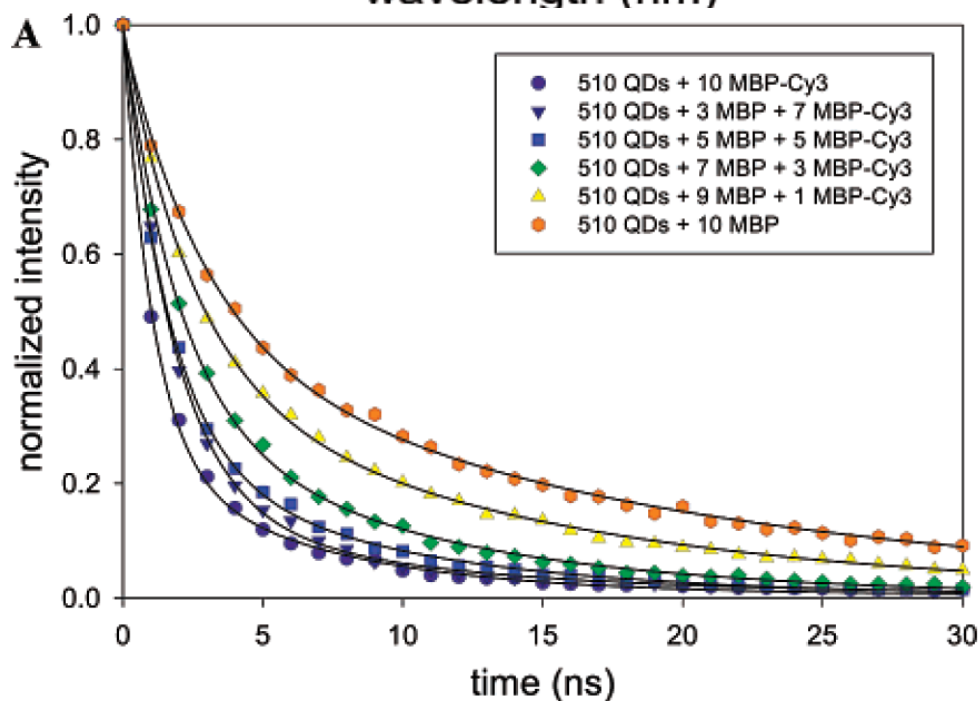
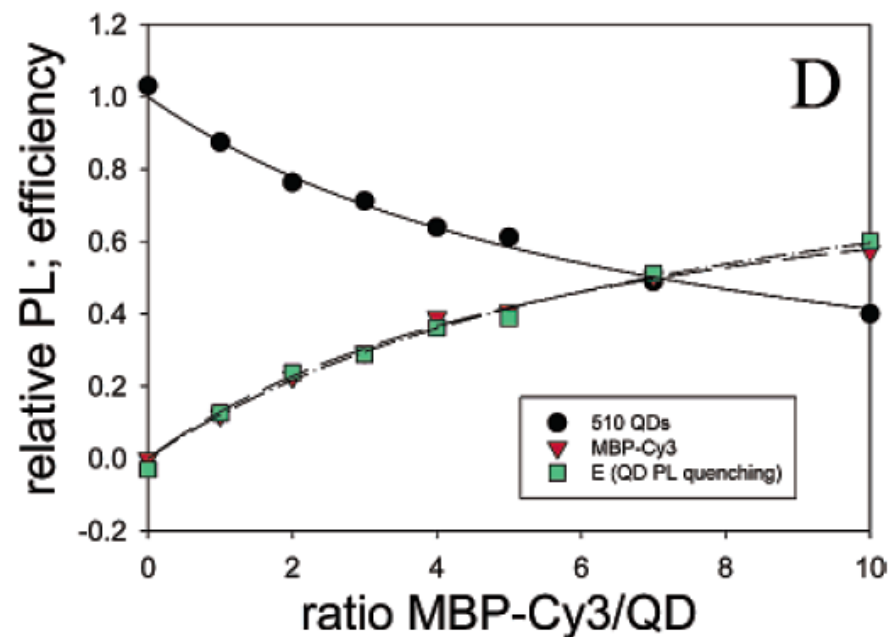
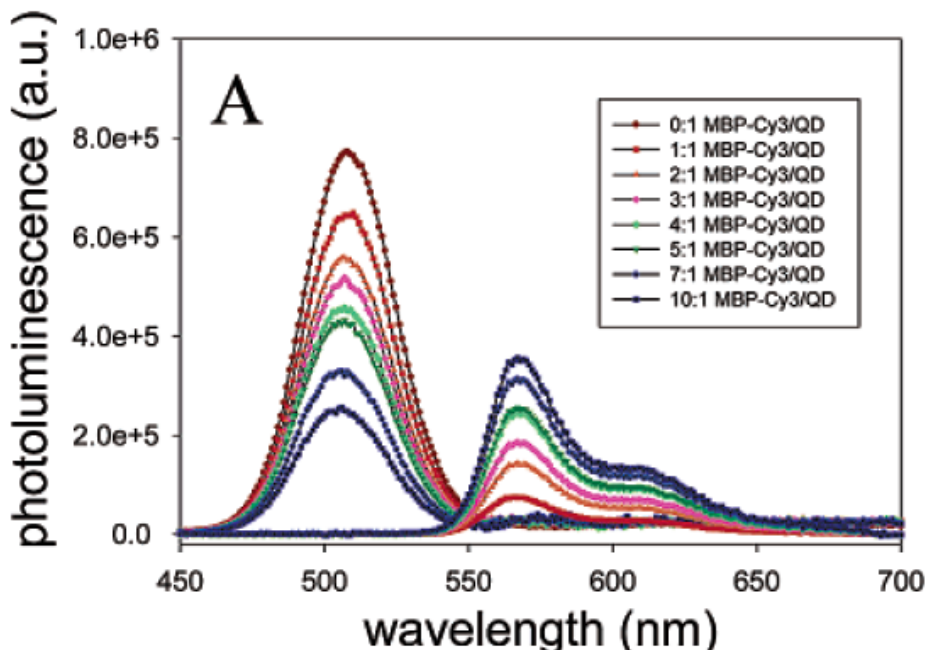
Table 1. Overlap Integrals, Quantum Yields, and Calculated Förster Distances for MBP-Coated QD–Cy3 Pairs

donor–acceptor pair	overlap integral, $I \times 10^{13} (\text{cm}^3/\text{M})$	quantum yield, ^a Q_D	Förster distance, $R_0 (\text{Å})$
---------------------	---	-----------------------------------	------------------------------------

H. Mattoussi group, Naval Res. Lab
 A. R. Clapp et al.,
 J. Am. Chem. Soc. 126, 301 (2004)

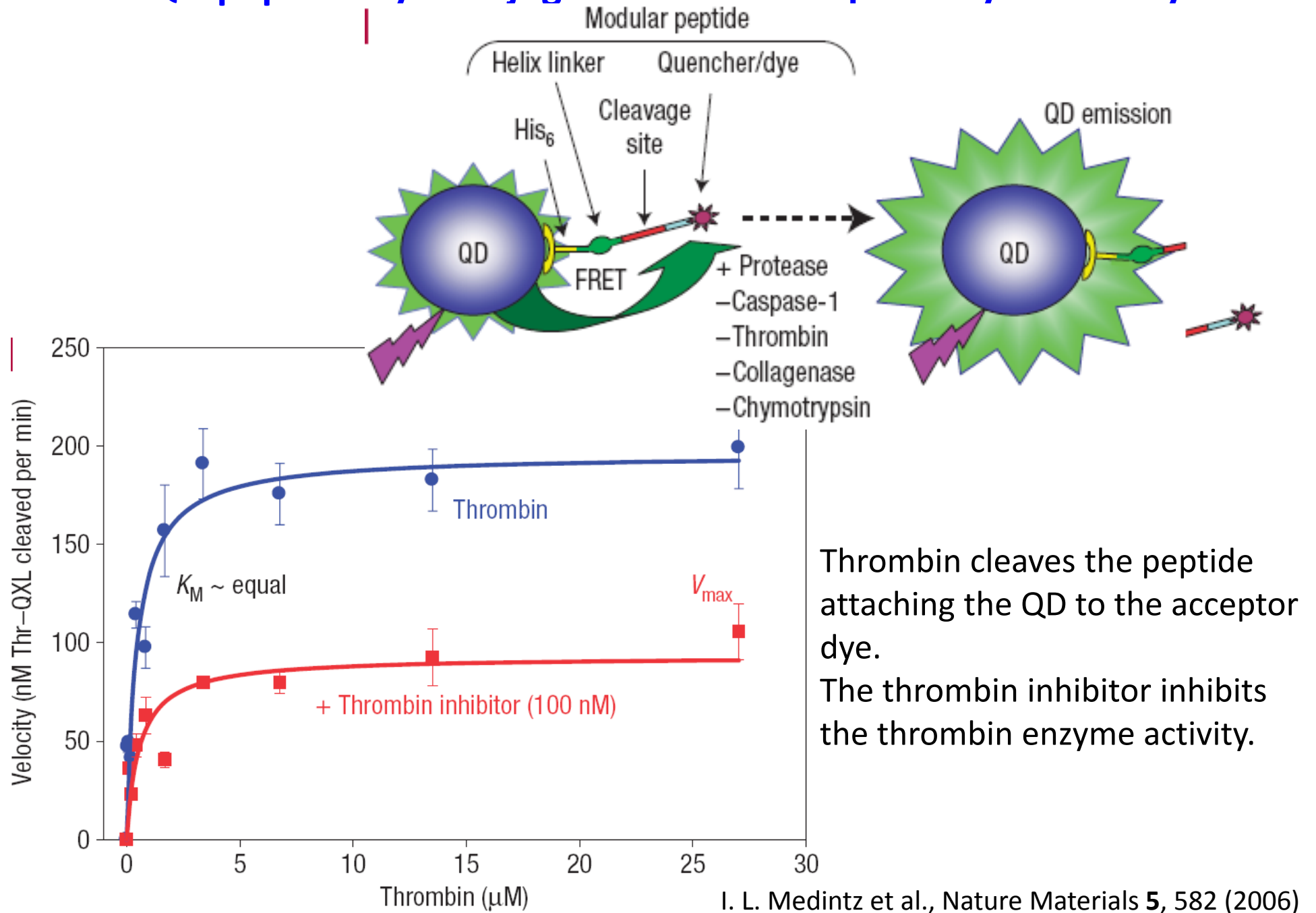
510–Cy3	3.86	0.190	47.3
530–Cy3	7.01	0.153	50.4
555–Cy3	8.91	0.239	56.5

Energy transfer from a QD donor to multiple organic acceptors

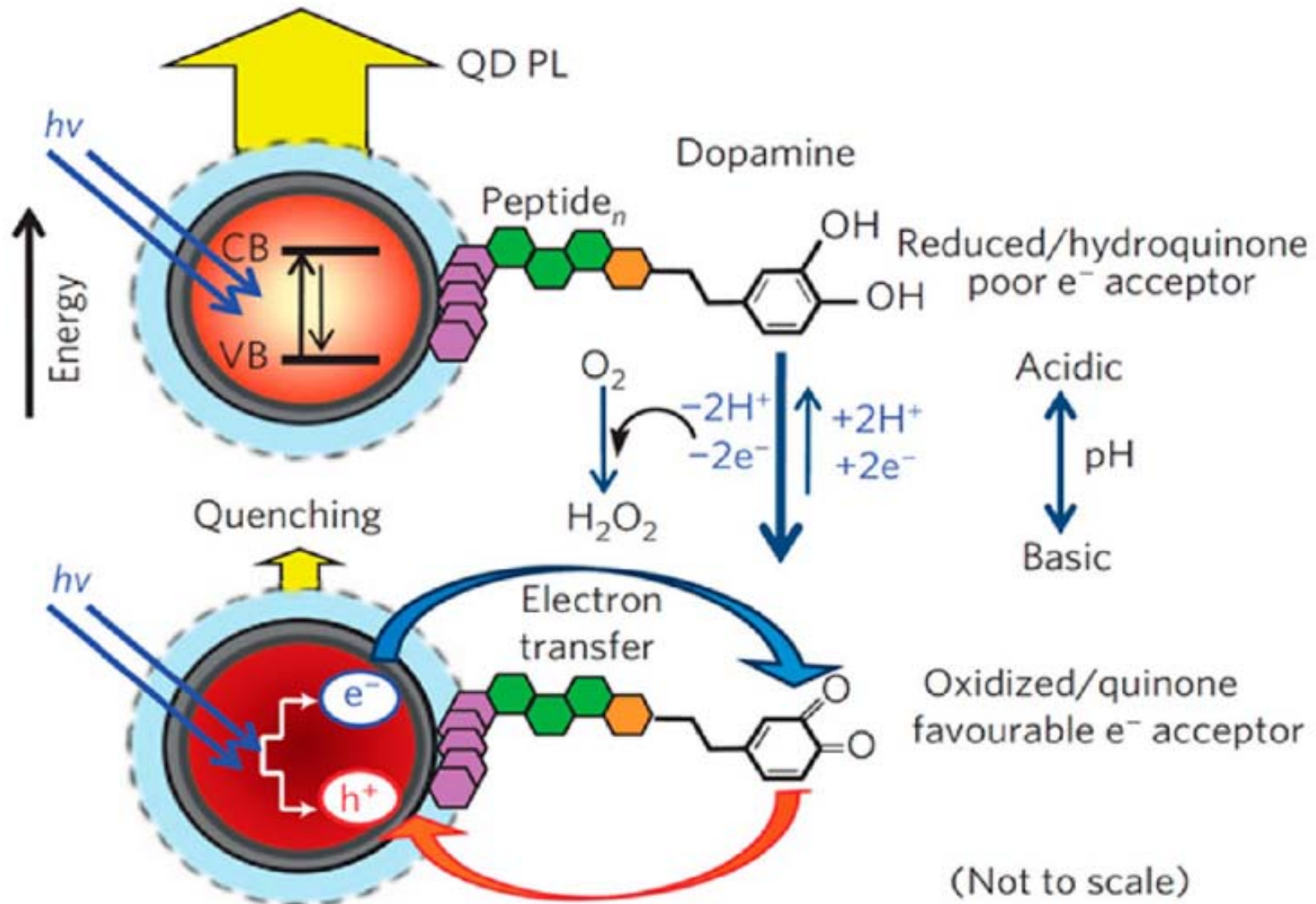


$$E = \frac{nR_0^6}{nR_0^6 + r^6}$$

QD-peptide-dye conjugates to monitor proteolytic activity

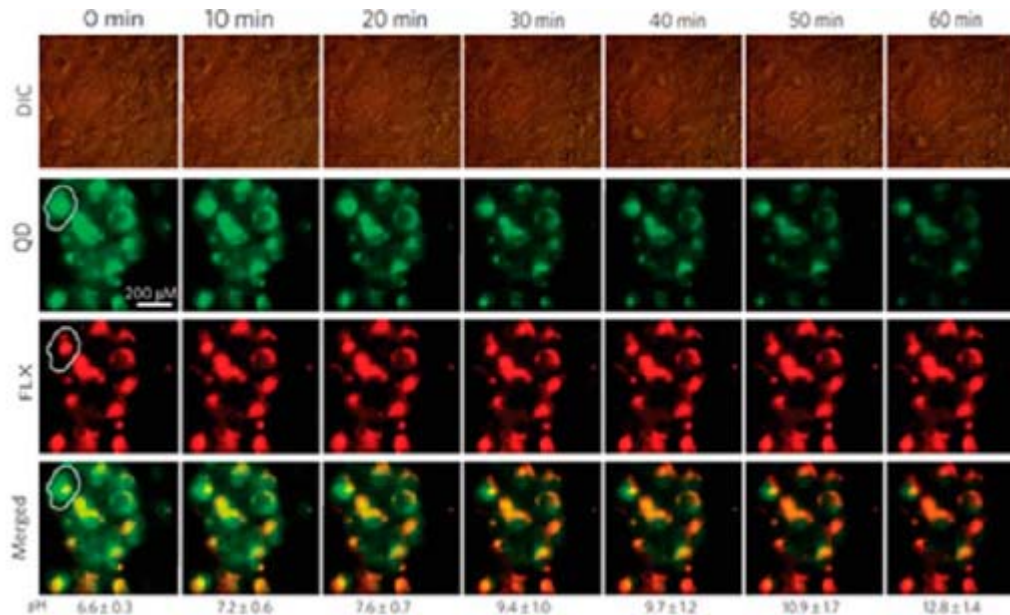


Sensing pH changes with QDs + FRET



Medintz, I. L., Mattoussi, H. et al., Quantum-Dot/Dopamine Bioconjugates Function as Redox Coupled Assemblies for in Vitro and Intracellular pH Sensing. Nat. Mater. 2010, 9, 676–684.

Sensing pH changes



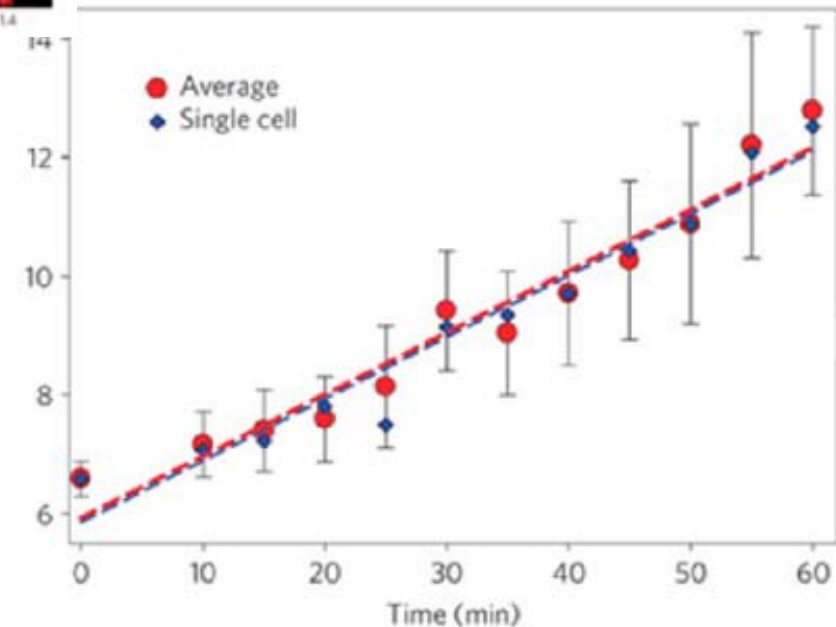
COS-1 cells + nystatin

-> intracellular pH changes

Green : QD-dopamine conjugates

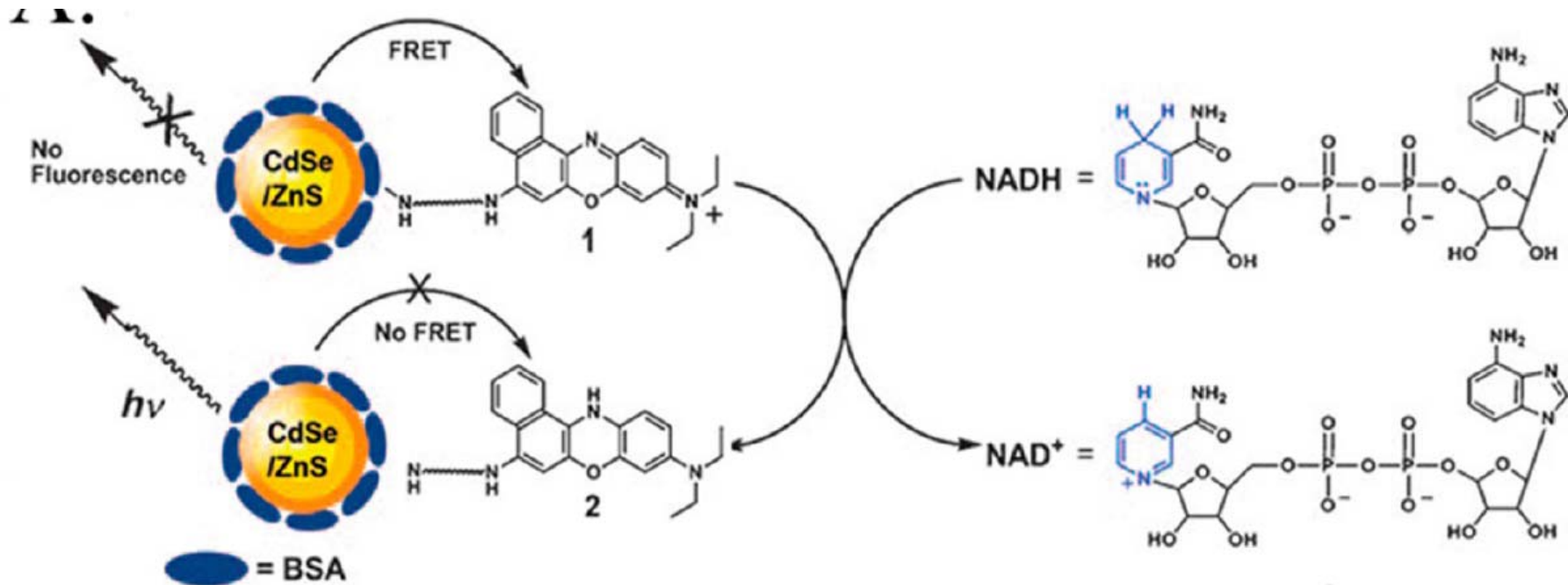
Red : nanospheres incorporating red organic fluorophores

Medintz, I. L., Mattoussi, H. et al.,
Quantum-Dot/Dopamine Bioconjugates
Function as Redox Coupled Assemblies
for in Vitro and Intracellular pH
Sensing. Nat. Mater. 2010, 9, 676–684.



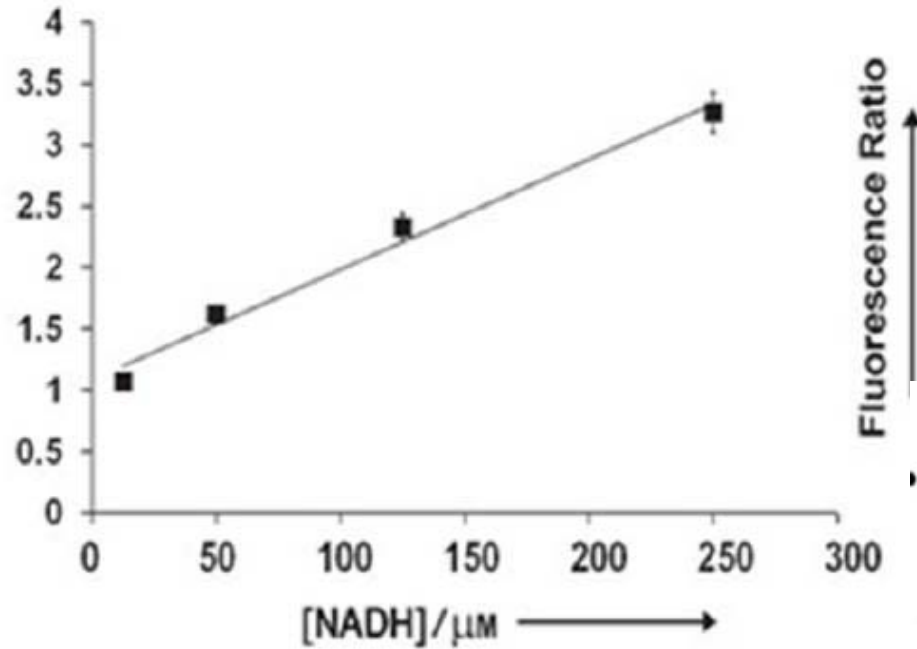
Measuring intracellular NADH concentrations

NADH indicates cell metabolic activity



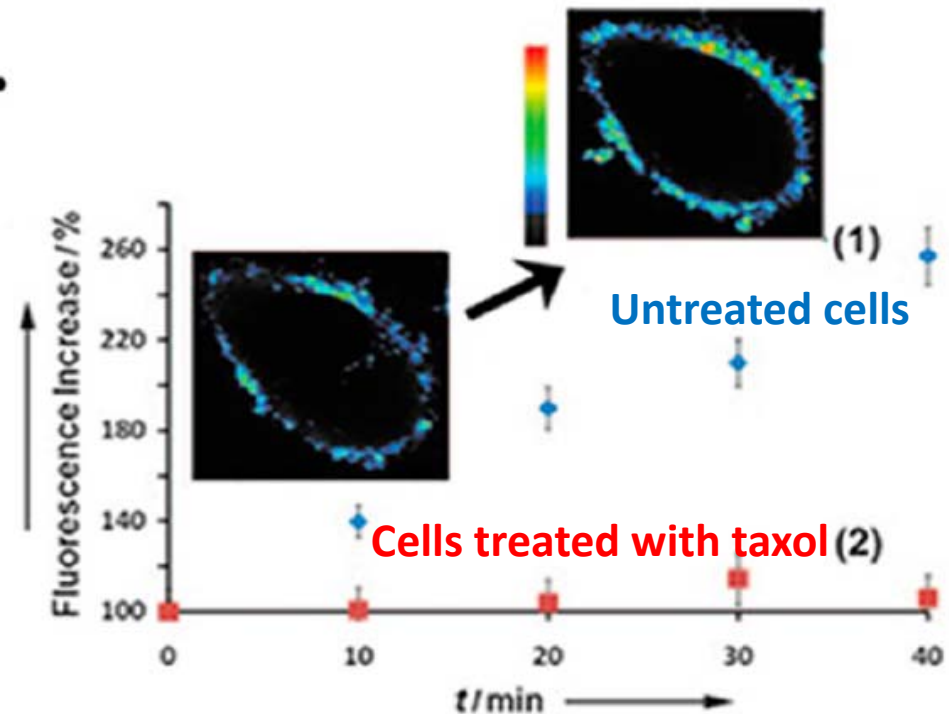
Freeman, R.; Gill, R.; Shweky, I.; Kotler, M.; Banin, U.; Willner, v I. Biosensing and Probing of Intracellular Metabolic Pathways by NADH-Sensitive Quantum Dots. *Angew. Chem., Int. Ed.* 2009, 48, 309–313.

Measuring intracellular NADH concentrations

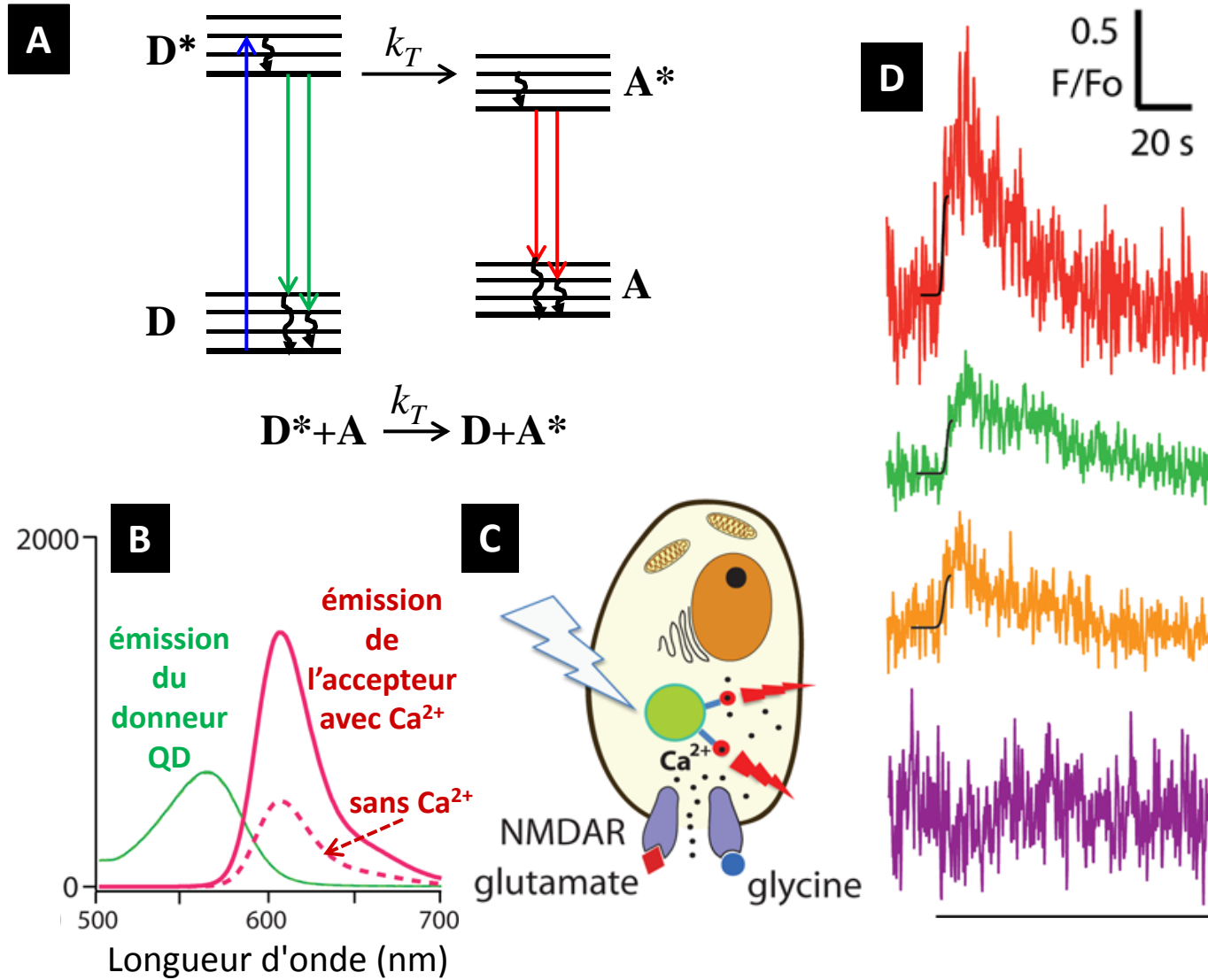


Evaluate effects of drug treatment

HeLa cancer cells + 50 nM glucose



Sensing Ca^{2+} with QDs and energy transfer (FRET)

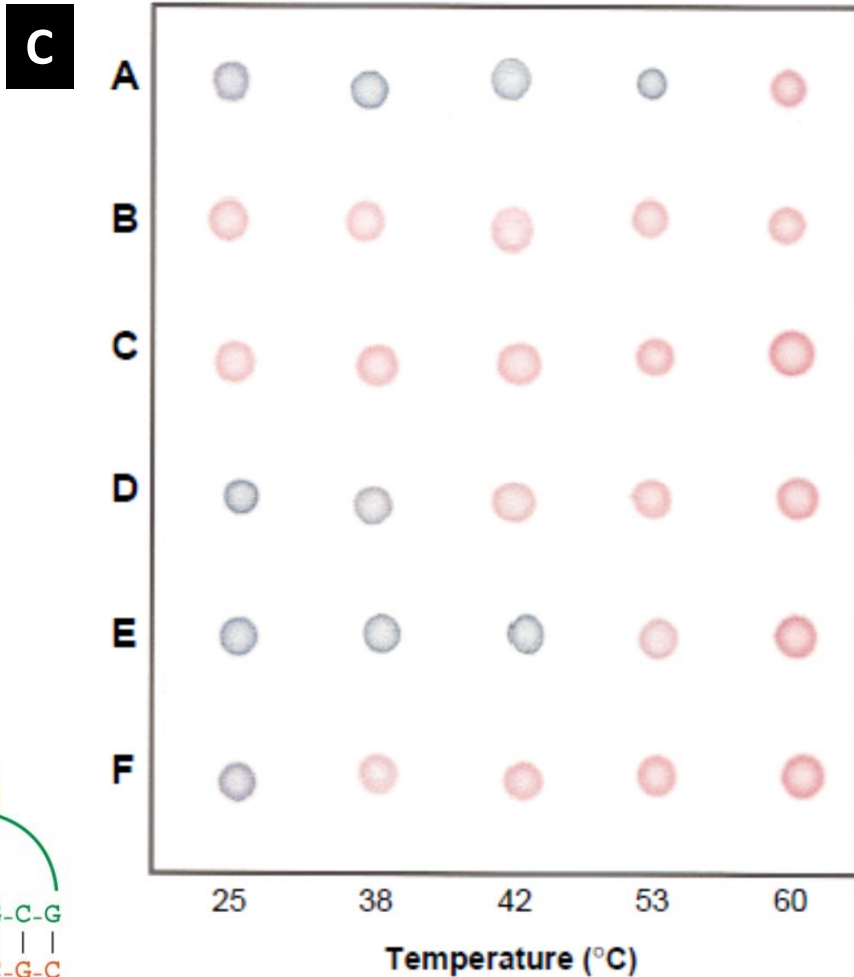
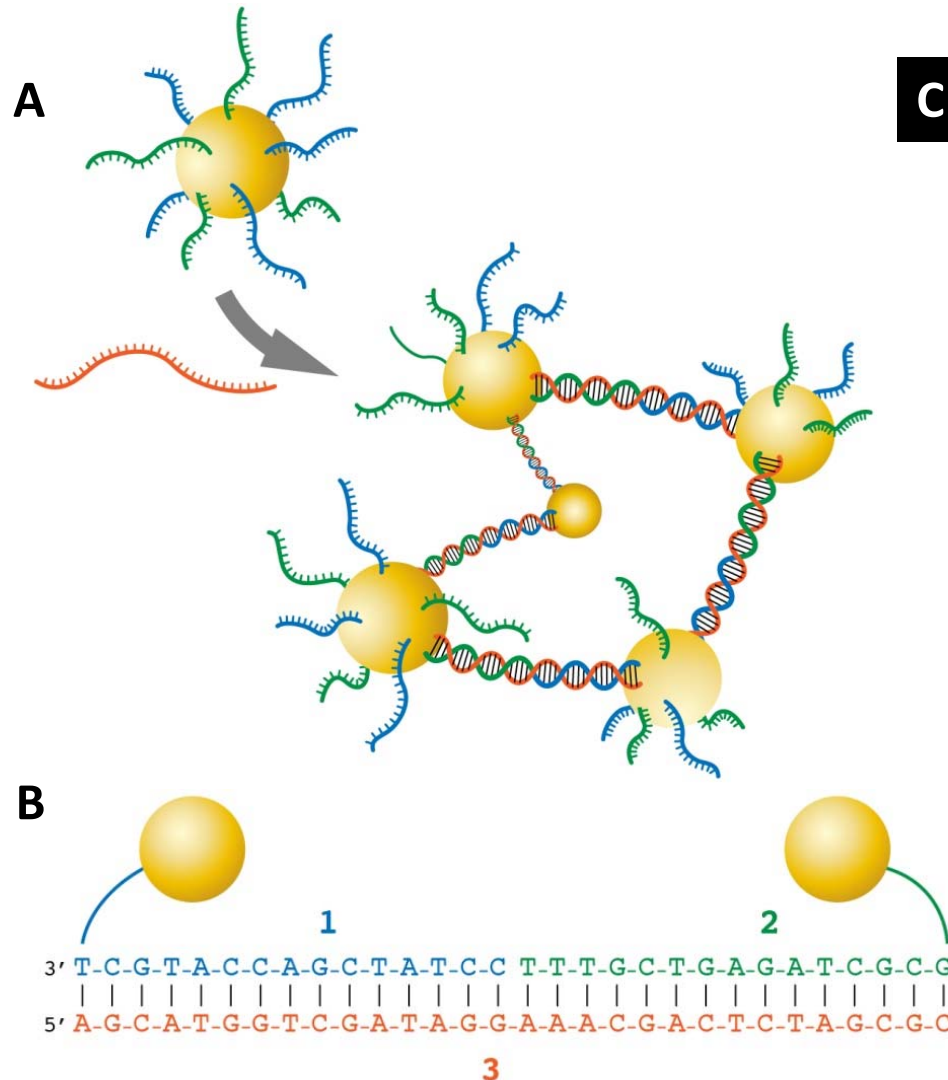


Zamaleeva et al., *Nano Lett.* 14, 2994 (2014).

***In vitro* diagnostics**

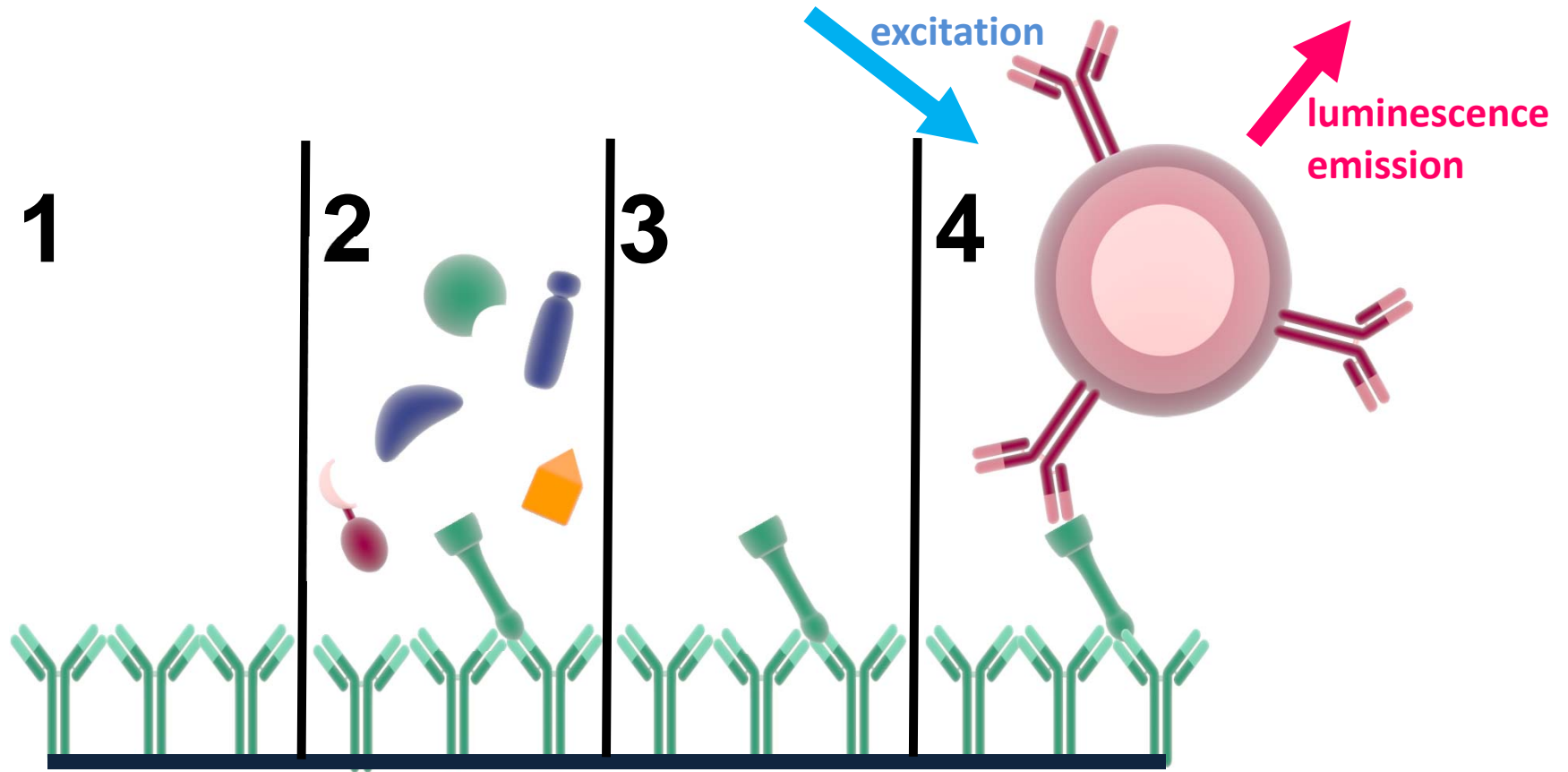
In vitro diagnostics with gold nanoparticles

Based on **surface plasmons**: collective electron oscillations



Mirkin et al., Science 277, 1078 (1997).

In vitro diagnostics with luminescent nanoparticles

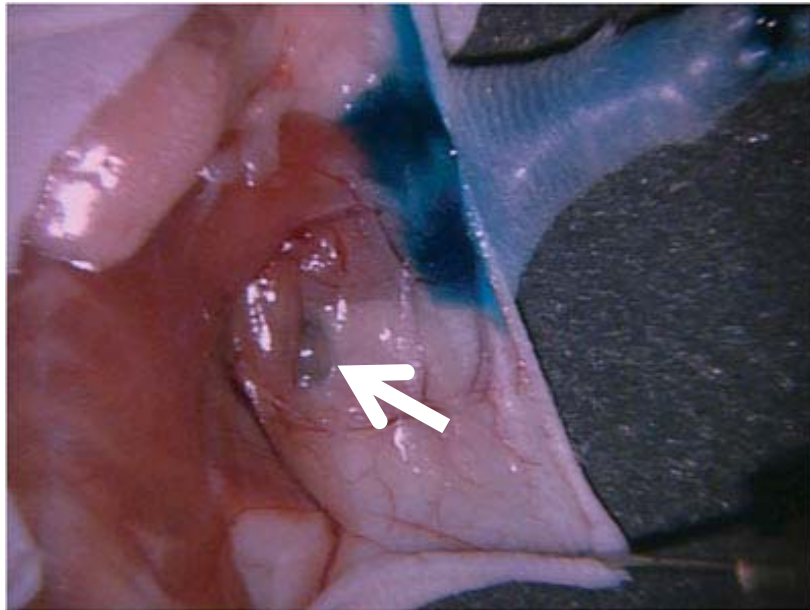


Start-up project at Ecole polytechnique with M. Richly, C. Bouzigues, P. Pereira, AA

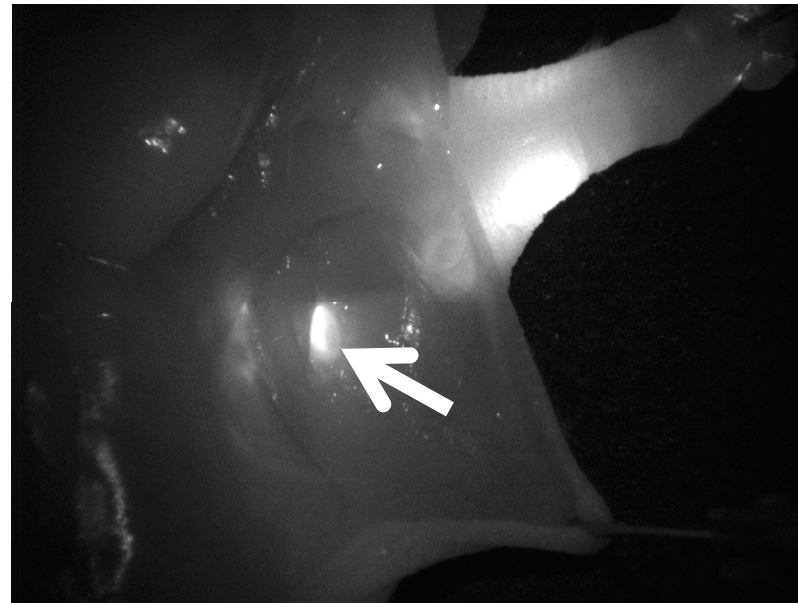
***In vivo* applications**

***In vivo* applications**
Peroperative sentinel lymph node imaging
with near-infrared Quantum Dots

Color video

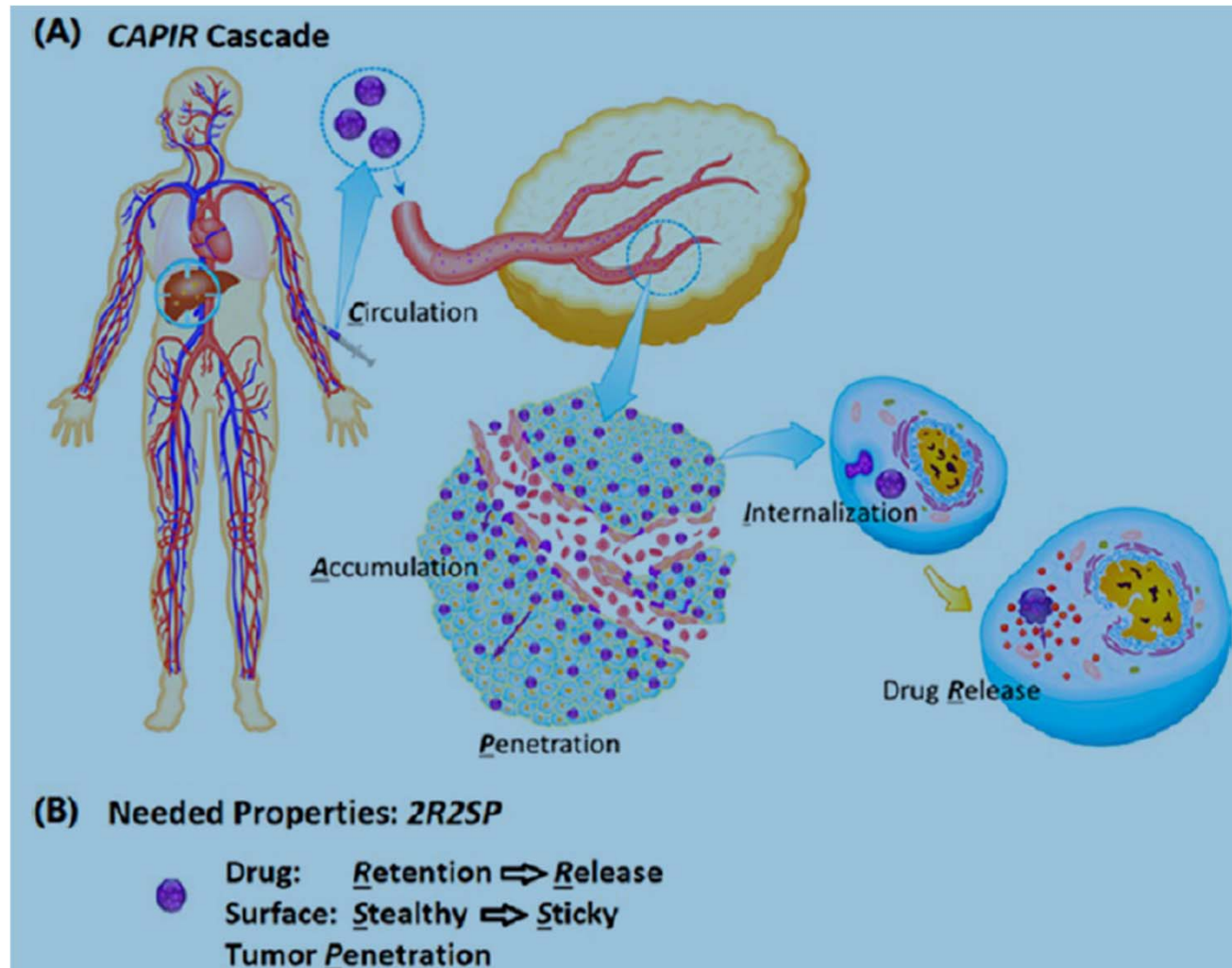


Near-infrared luminescence



In vivo applications

Nanoparticle-based drug delivery

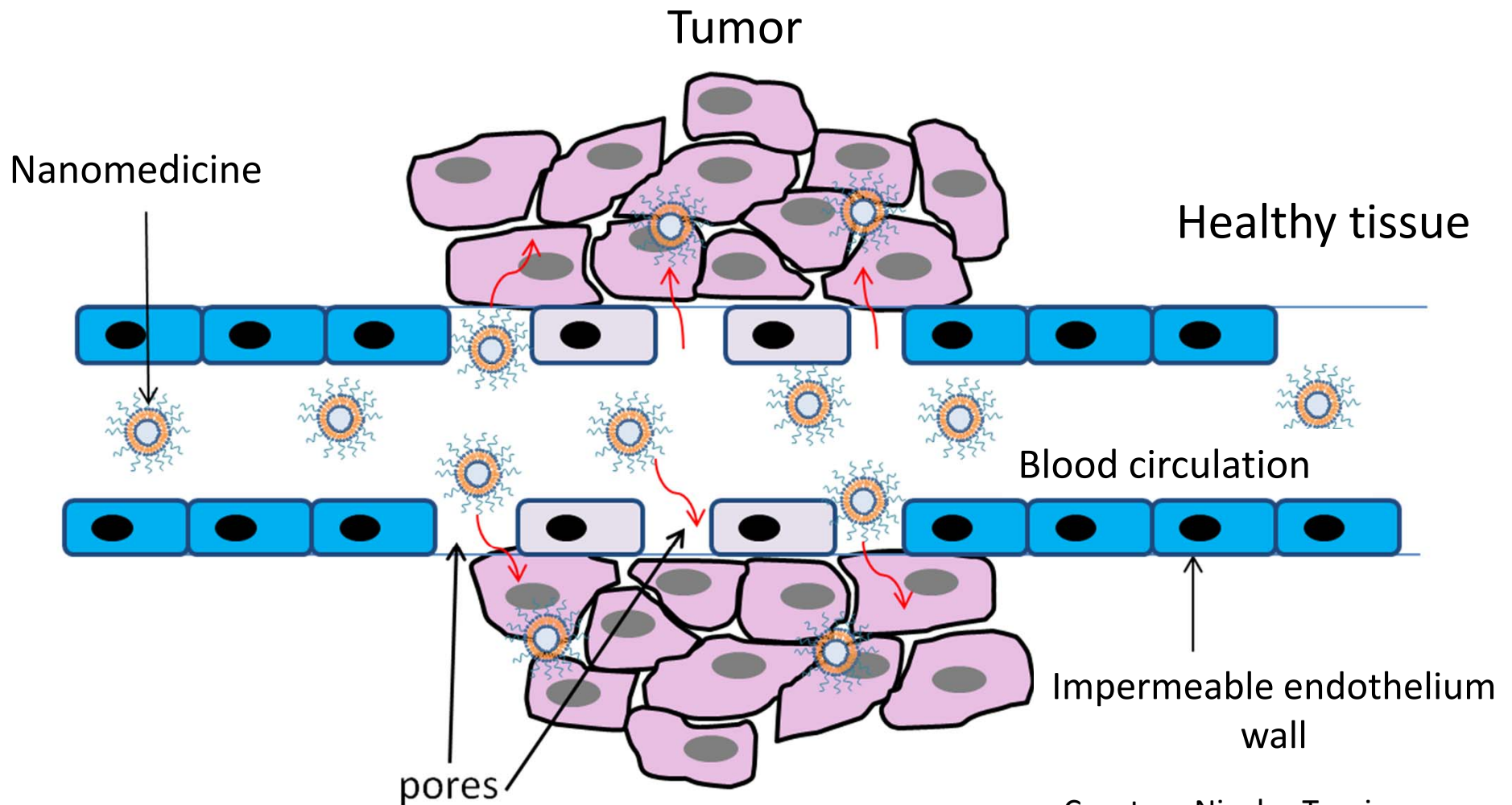


Sun, Q. H.; Sun, X. R.; Ma, X. P.; Zhou, Z. X.; Jin, E. L.; Zhang, B.; Shen, Y. Q.; Van Kirk, E. A.; Murdoch, W. J.; Lott, J. R.; Lodge, T. P.; Radosz, M.; Zhao, Y. L. Integration of Nanoassembly Functions for an Effective Delivery Cascade for Cancer Drugs. *Adv. Mater.* 2014, 26, 7615–7621.

Nanoparticles for drug delivery

Passive drug delivery

Enhanced permeabilization and retention (EPR) in tumors

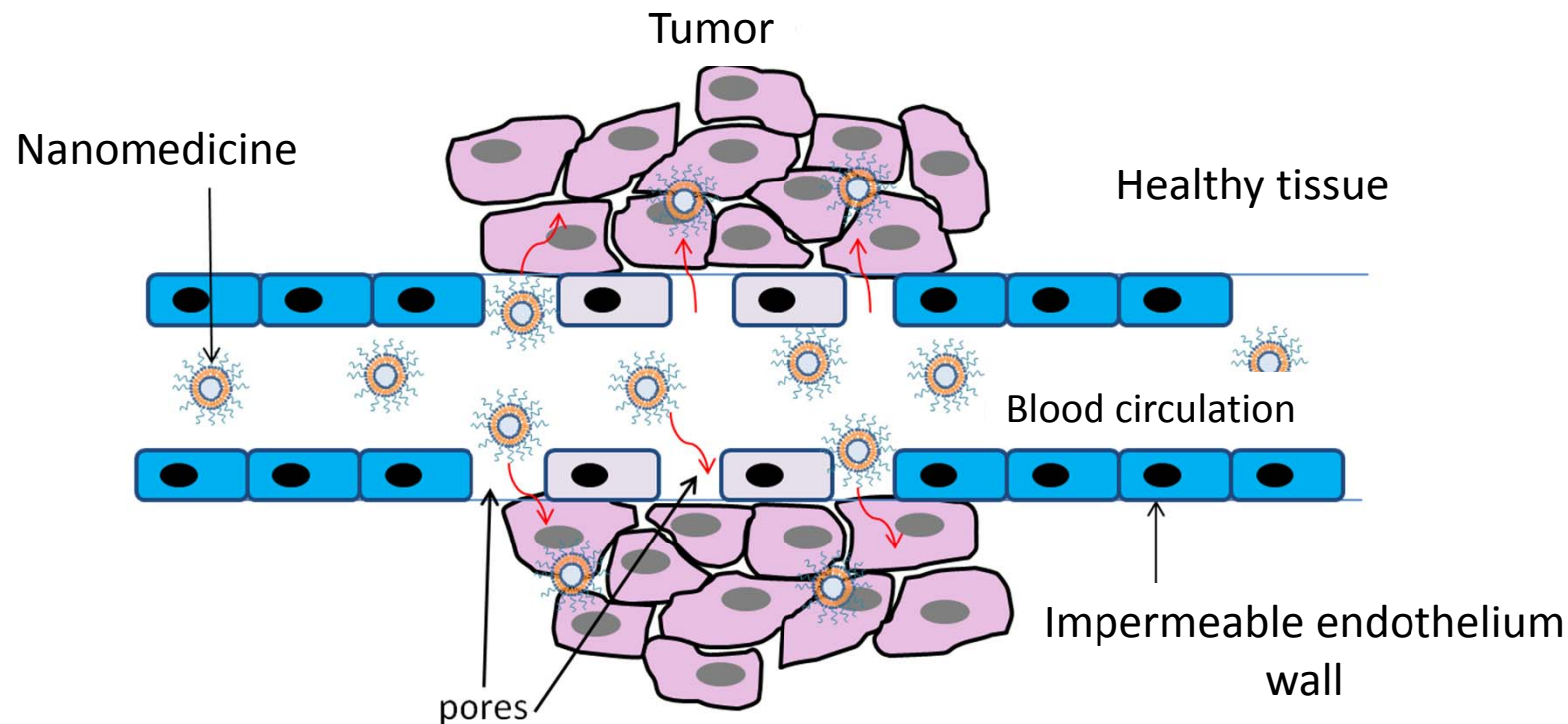


Courtesy Nicolas Tsapis

Nanoparticles for drug delivery

Passive drug delivery

Enhanced permeabilization and retention (EPR) in tumors



Small organic molecules (chemotherapy drugs) can reach both healthy and tumoral tissues.

Nanoparticles (30-50 nm) can leave the blood circulation only when the blood cell wall is permeable.

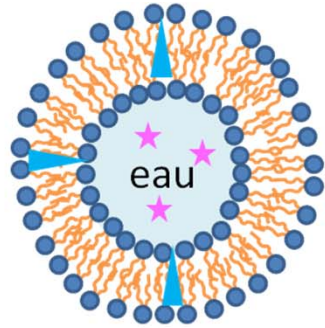
-> Nanoparticles preferentially enter tumoral tissue

Less side effects

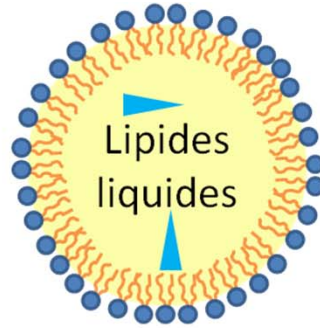
Lower dosages necessary

Nanoparticles for drug delivery

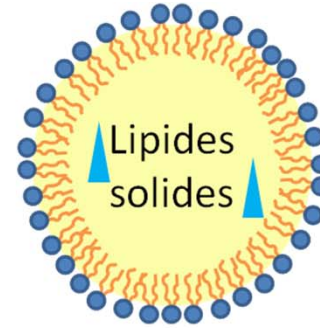
Drug nanocarriers must be biocompatible



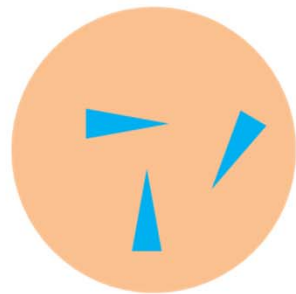
Liposome



Micelle



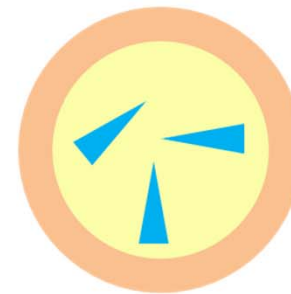
Nanoparticule
lipidique solide





Nanosphère





Nanocapsule
(coeur aqueux)



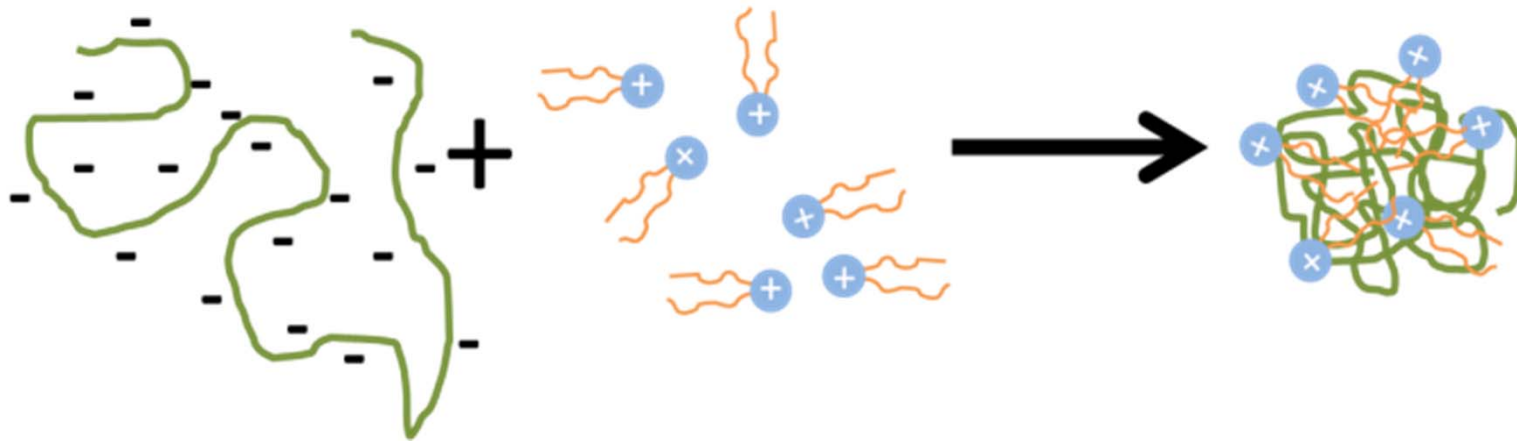
Nanocapsule
(coeur huileux)

 Matrice polymère
 Phospholipide

 Substance active hydrophobe
 Substance active hydrophile

Polymeric nanoparticles

Condensing nucleic acids (DNA, RNA) with positively charged cationic lipids to form nanoparticles



Inside a nanoparticle, nucleic acids are protected from degradation.

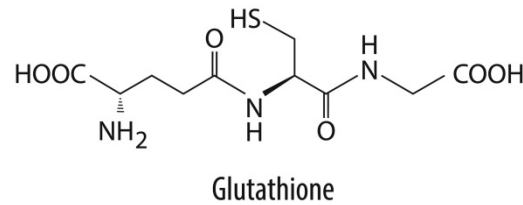
-> Gene therapy

Stimulus responsive drug release

Stimulus → **pH** (lower pH in the tumor microenvironment)

Protonation-deprotonation → destabilization/degradation of drug nanocarrier

Redox potential (2-10 mM glutathione (GSH) in healthy tissue, 10-25 mM in tumors)



Reactive oxygen species (ROS, e.g. H₂O₂) (Overexpressed in some tumors)

Wang, J. R.; Sun, X. R.; Mao, W. W.; Sun, W. L.; Tang, J. B.; Sui, M. H.; Shen, Y. Q.; Gu, Z. W. Tumor Redox Heterogeneity-Responsive Prodrug Nanocapsules for Cancer Chemotherapy. *Adv. Mater.* 2013, 25, 3670–3676.



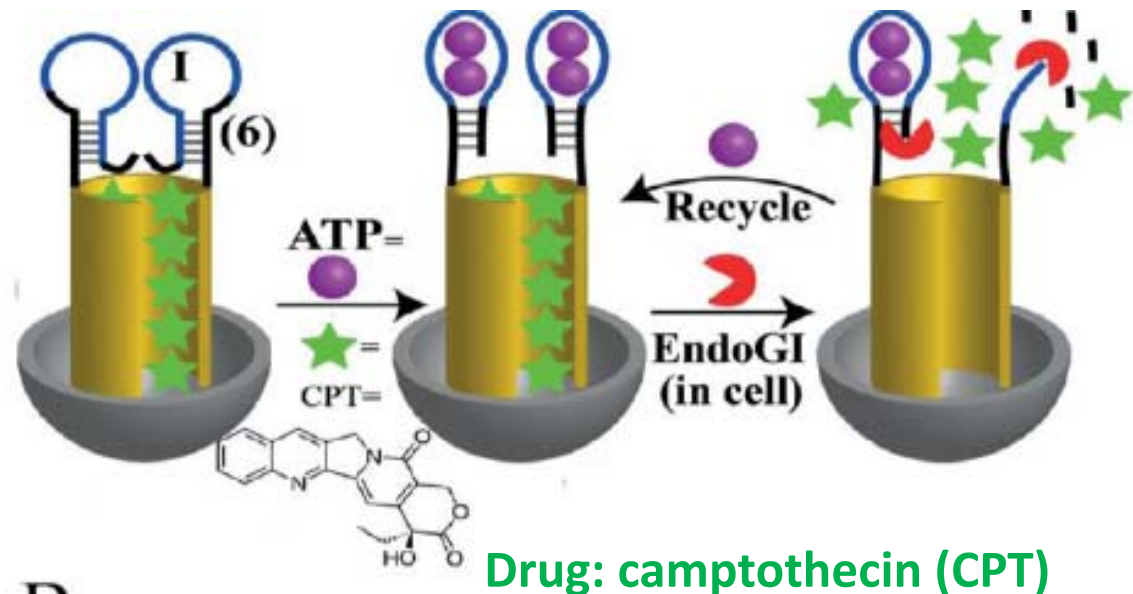
Stimulus responsive drug release

Stimulus

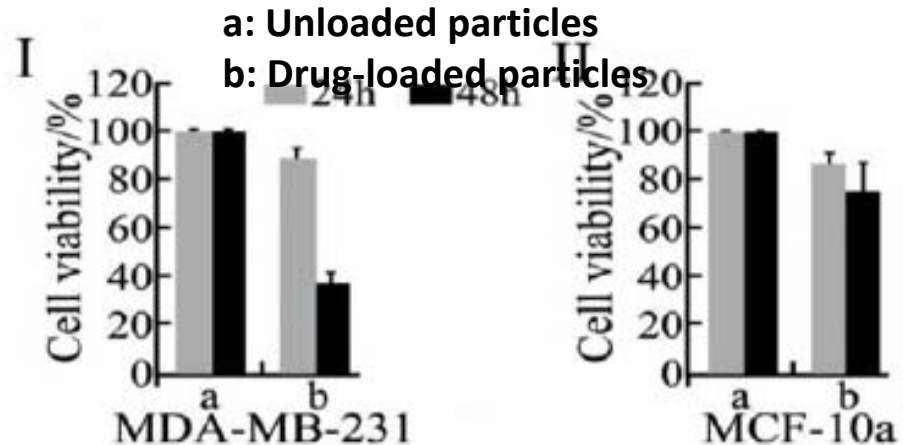


Enzymes (in abundance in pathological conditions, e.g. matrix metalloproteinases, exonucleases)

High concentrations of ATP and endonuclease EndoGI in tumor cells.



B.

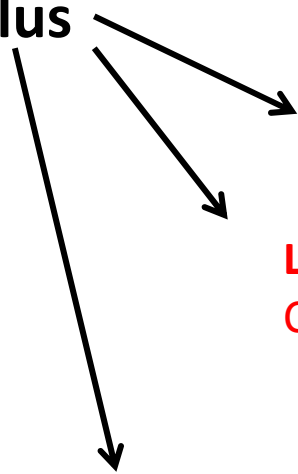


Breast cancer cells

Normal breast cells

Stimulus-responsive drug release

Stimulus



Heat (stable at 37°C, rapid degradation of nanocarrier at 40-42°C)

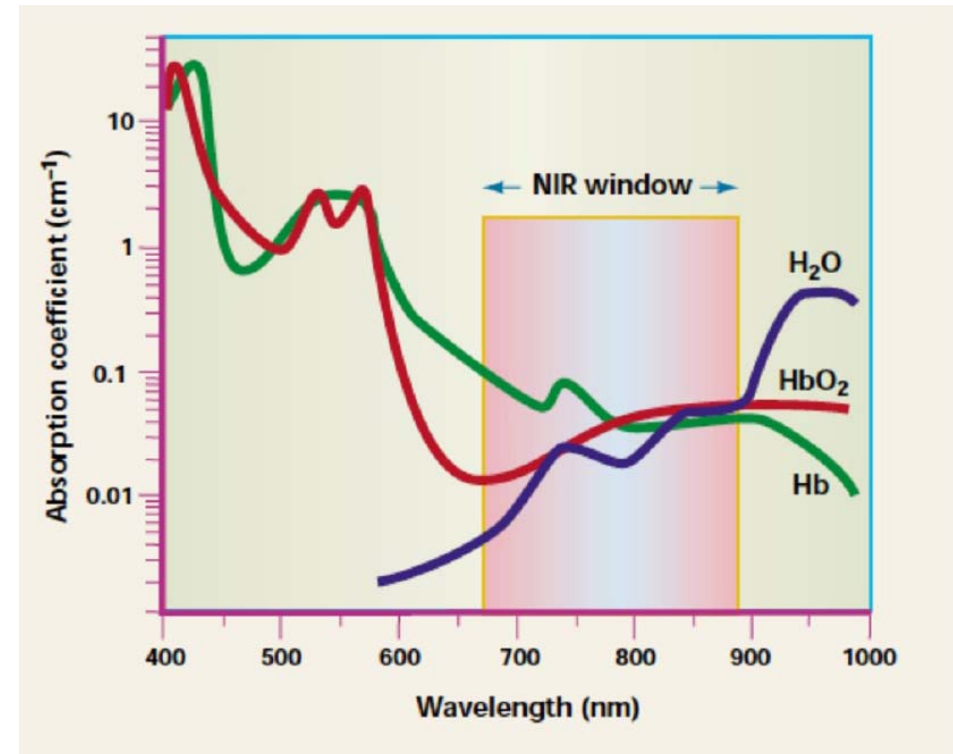
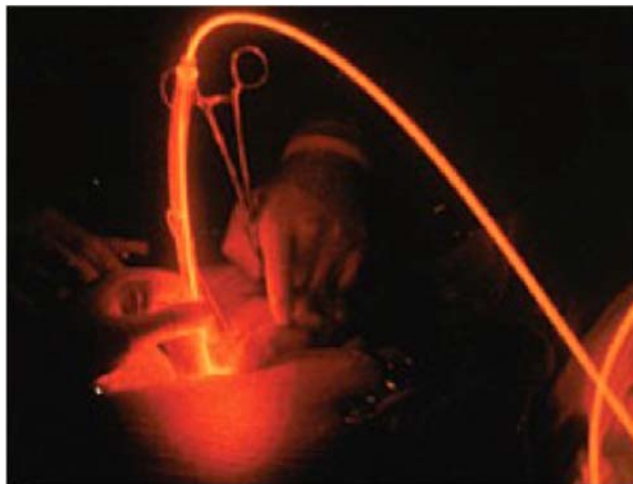
Light (polymer-based drug nanocarriers containing Au NPs)
Controlled release of heat to degrade nanocarrier

If deep tissue penetration is required: near-IR light

....

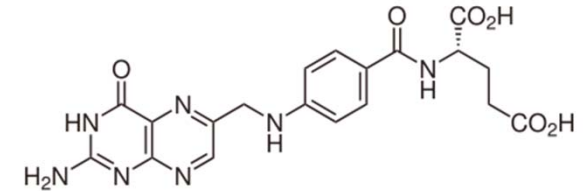
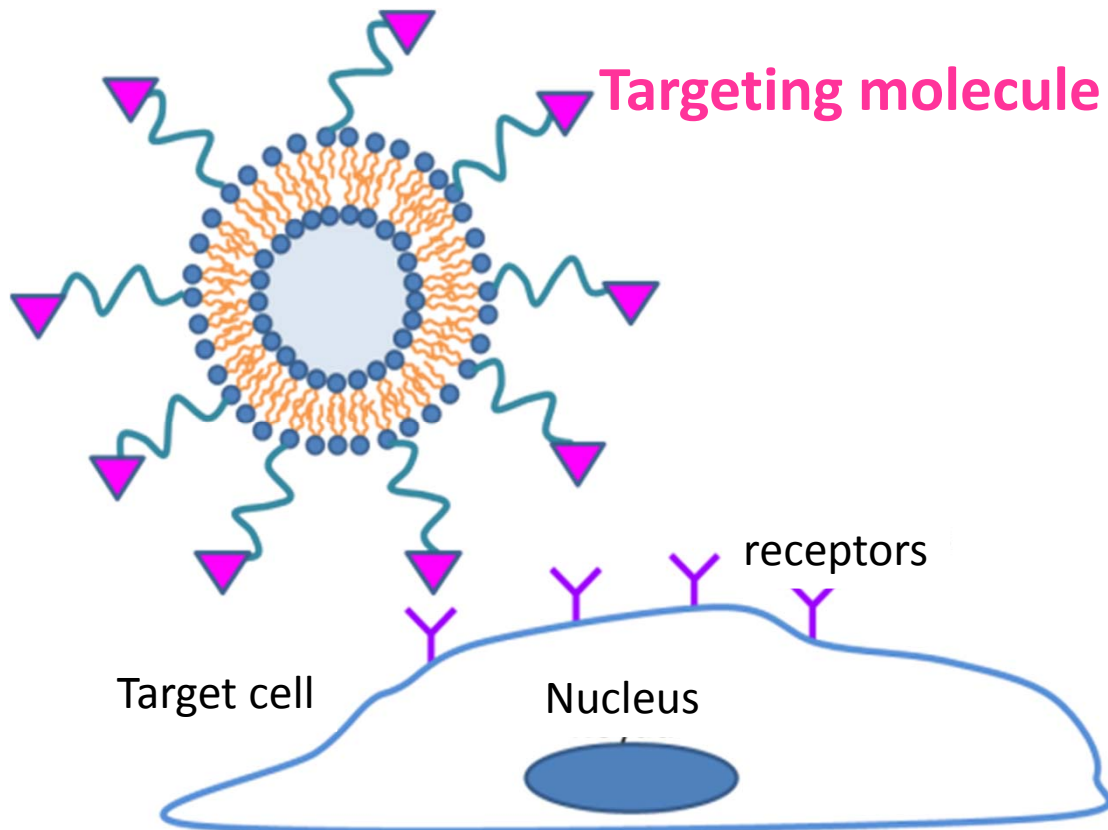
Endoscopic tools
and optical fibers

During surgery



Nanoparticles for drug delivery

Active drug delivery



Folic acid (vitamin B9)
Necessary for DNA replication
Overexpressed in tumor cells

...

**Controversy about efficacy
of active targeting**

Nanoparticles for drug delivery

Localized drug delivery

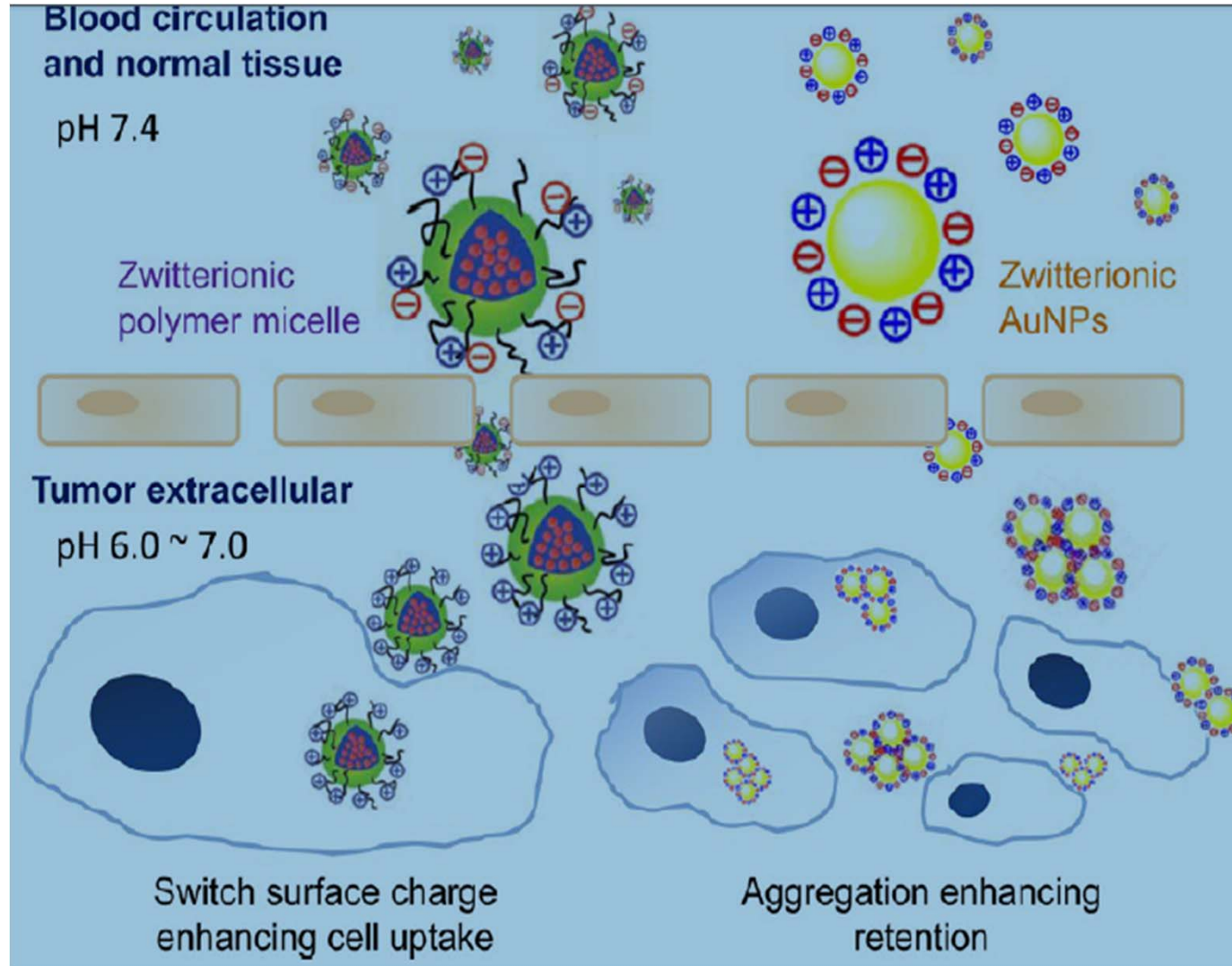
How ?



External magnetic field

Nanoparticles for drug delivery

Stealthy to sticky transformation

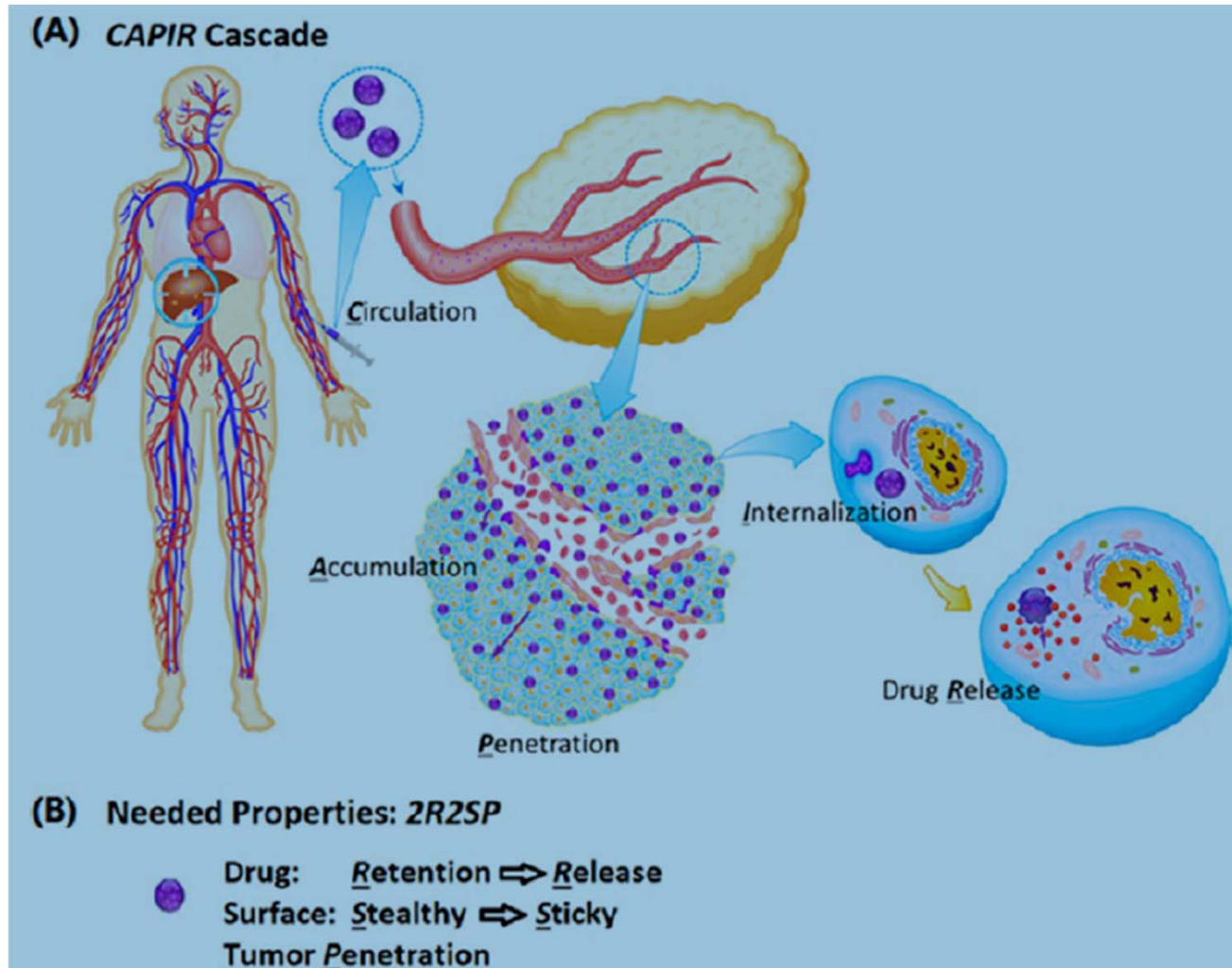


Yuan, et al. , Surface Charge Switchable Nanoparticles Based on Zwitterionic Polymer for Enhanced Drug Delivery to Tumor. *Adv. Mater.* 2012, 24, 5476–5480.

Liu, X. SJ. Surface Tailoring of Nanoparticles via Mixed-Charge Monolayers and Their Biomedical Applications. *Small* 2014, 10, 4230–4242.

In vivo applications

Nanoparticle-based drug delivery



Sun, Q. H.; Sun, X. R.; Ma, X. P.; Zhou, Z. X.; Jin, E. L.; Zhang, B.; Shen, Y. Q.; Van Kirk, E. A.; Murdoch, W. J.; Lott, J. R.; Lodge, T. P.; Radosz, M.; Zhao, Y. L. Integration of Nanoassembly Functions for an Effective Delivery Cascade for Cancer Drugs. *Adv. Mater.* 2014, 26, 7615–7621.

Therapy with inorganic nanoparticles

Killing cells with external stimuli

Photodynamic therapy: Photosensitizers (type I, electron transfer; type II, singlet oxygen generation)

Desired properties: high absorption coefficient, triplet state with appropriate energy to interact with triplet oxygen ($S=1$), high transfer efficiency to the triplet state, long lifetime of triplet state, high photostability, low dark cytotoxicity (aromatic hydrocarbons, quinones, porphyrins, transition metal complexes like $[\text{Ru}(\text{bpy})_3]^{2+}$, ...)

Using nanoparticles allows targeted delivery of photosensitizers

Plasmonic hyperthermia: Au NPs, nanoshells, nanorods, ... + light

Light absorption due to surface plasmons

N. B. Protein adsorption on the Au NPs modifies plasmon properties

Magnetic hyperthermia: magnetic NPs + external alternating magnetic fields

Typically iron oxide NPs

Mechanical rotation of the whole NPs (Brown relaxation)

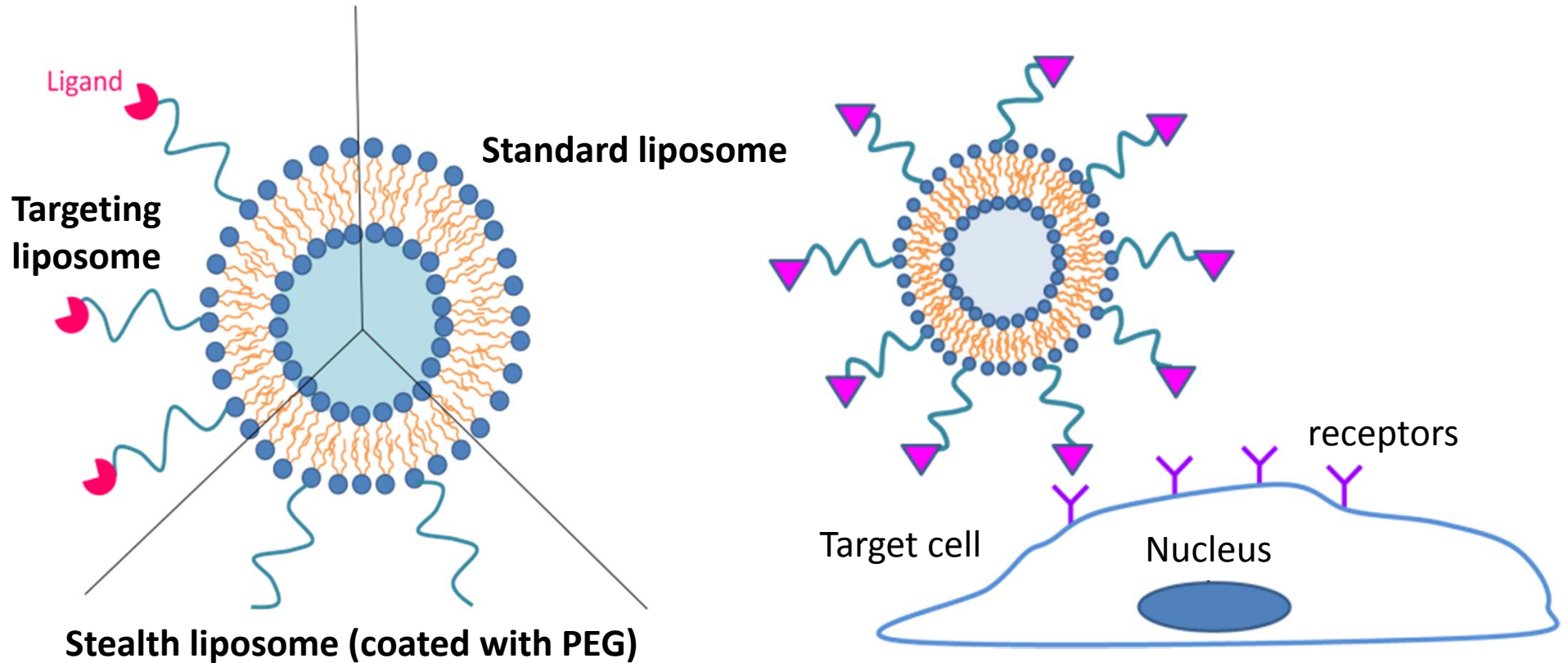
Rotation of the magnetic moment inside the core (Néel relaxation)

N. B. Aggregation of NPs reduces heating effect

Typically heating effects are smaller in cells than in water.

Biocompatible nanoparticles for drug delivery

Passive and active drug delivery



Nanoparticle-sensitized radiation therapy

Tumor-selective radiosensitizers (EPR effect)

X-ray radiation therapy: less invasive than surgery and chemotherapy

BUT : Both healthy and tumor tissues are exposed.

- Irradiate from multiple directions (multiport irradiation method)

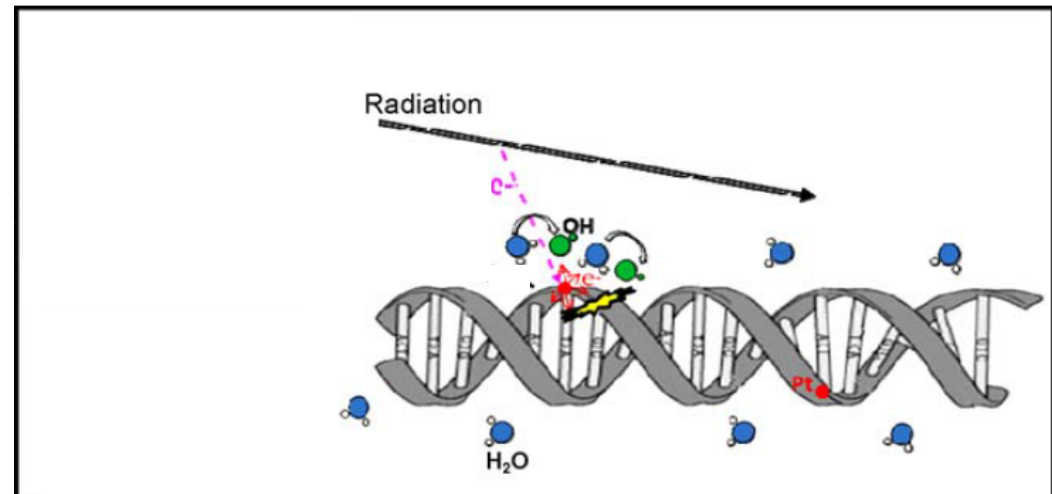
- **Use nanoparticles containing atoms that have large photoabsorption cross sections**

Enhance photoabsorption by tuning the energy of the X-rays to the absorption edge of the inner-shell electrons of these atoms

Photoionization + Auger deexcitation

Efficient DNA repair system in oxidative conditions

Unrepaired or mis-repaired DNA leads to cell death or genetic changes

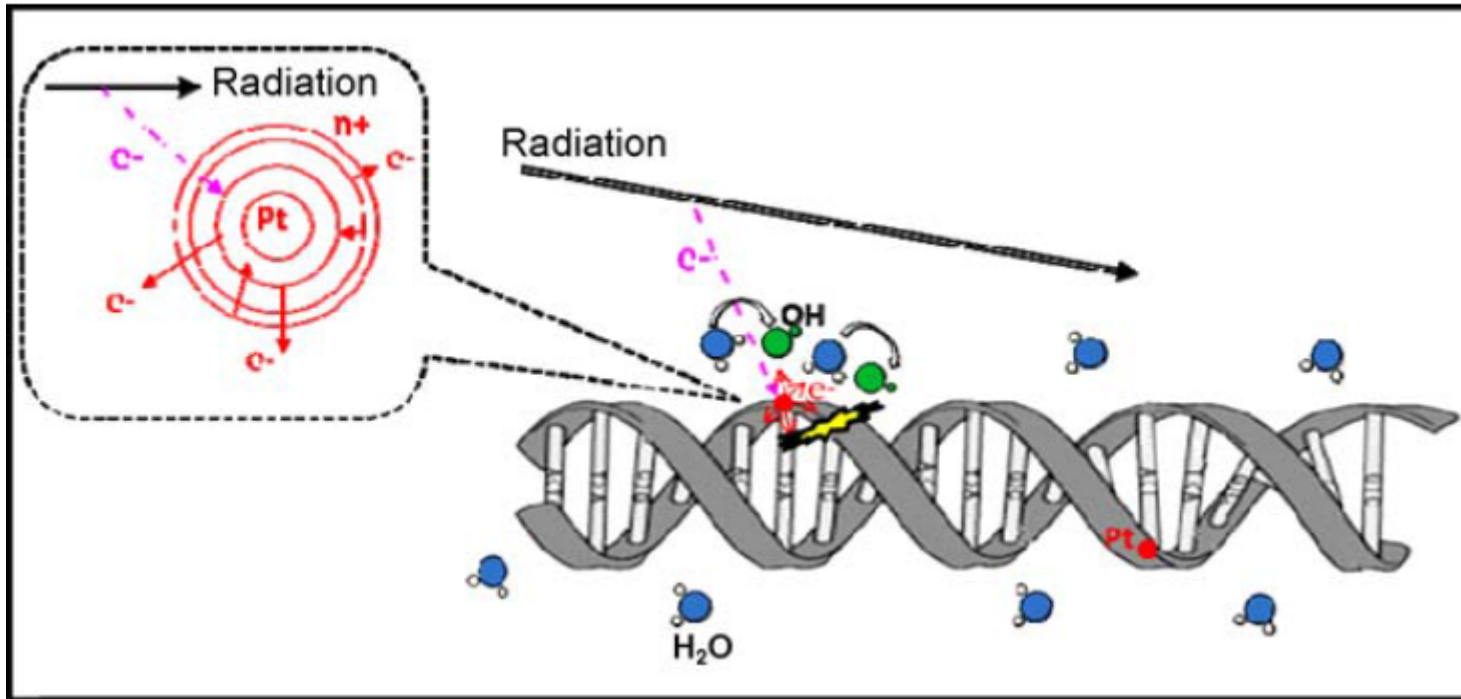


Selective production of a less repairable type of DNA damage

High linear energy transfer LET (in keV/ μm) leads to clustered DNA damage more difficult to repair. High LET is usually obtained with heavy ion particles.

Nanoparticle-sensitized radiation therapy

Tumor-selective radiosensitizers (EPR effect)



X-ray radiation can also produce high linear energy transfer by using high-Z atoms.

High-Z atoms :

Higher total photoabsorption cross section

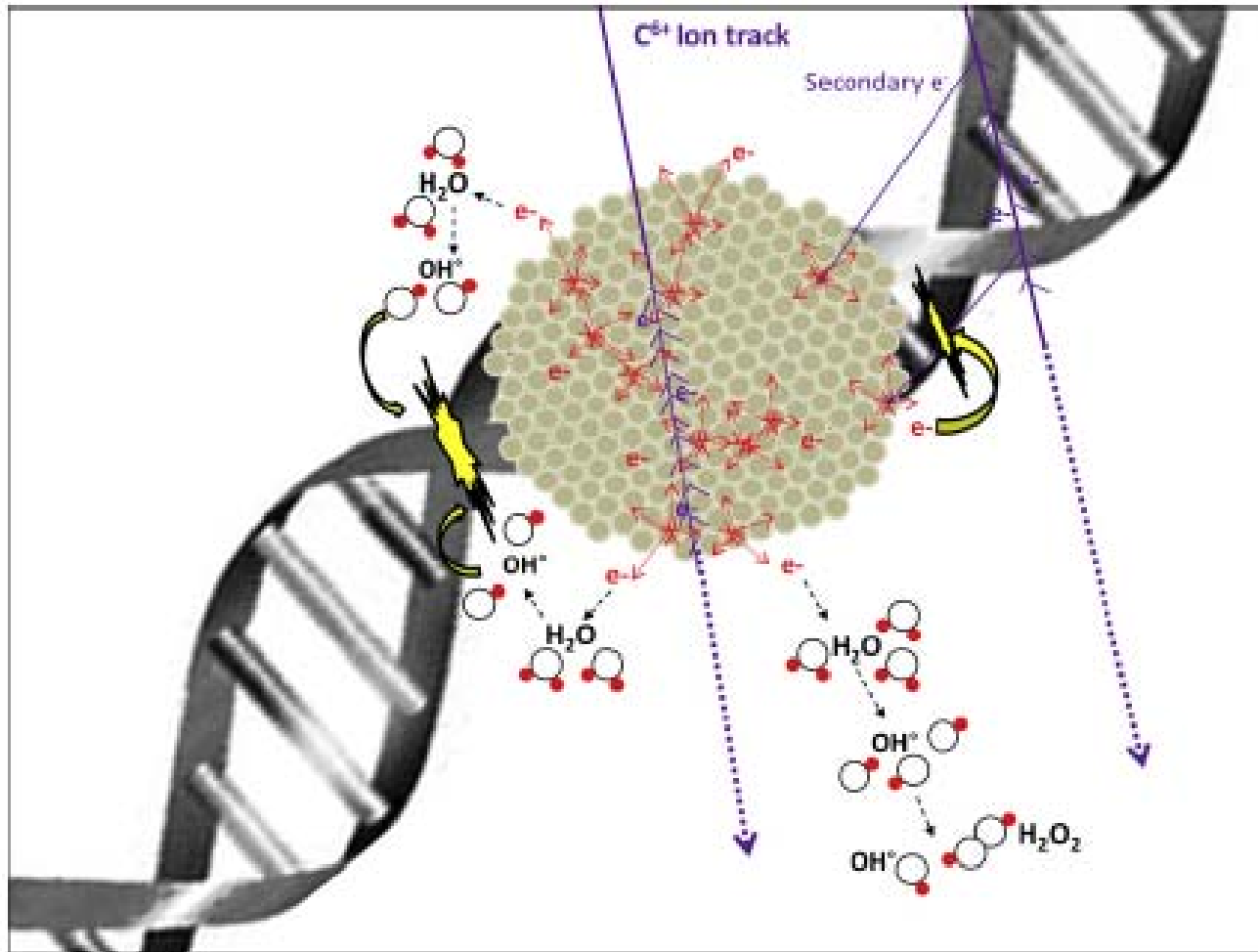
(Higher photoabsorption cross section for the inner-shell electrons)

Auger processes enhance the density of energy deposition events

Auger cascade, more Auger electrons are emitted from high Z-atoms (~30 from Pt after K-shell ionization)

-> Au, Pt NPs

Nanoparticle-sensitized hadron therapy

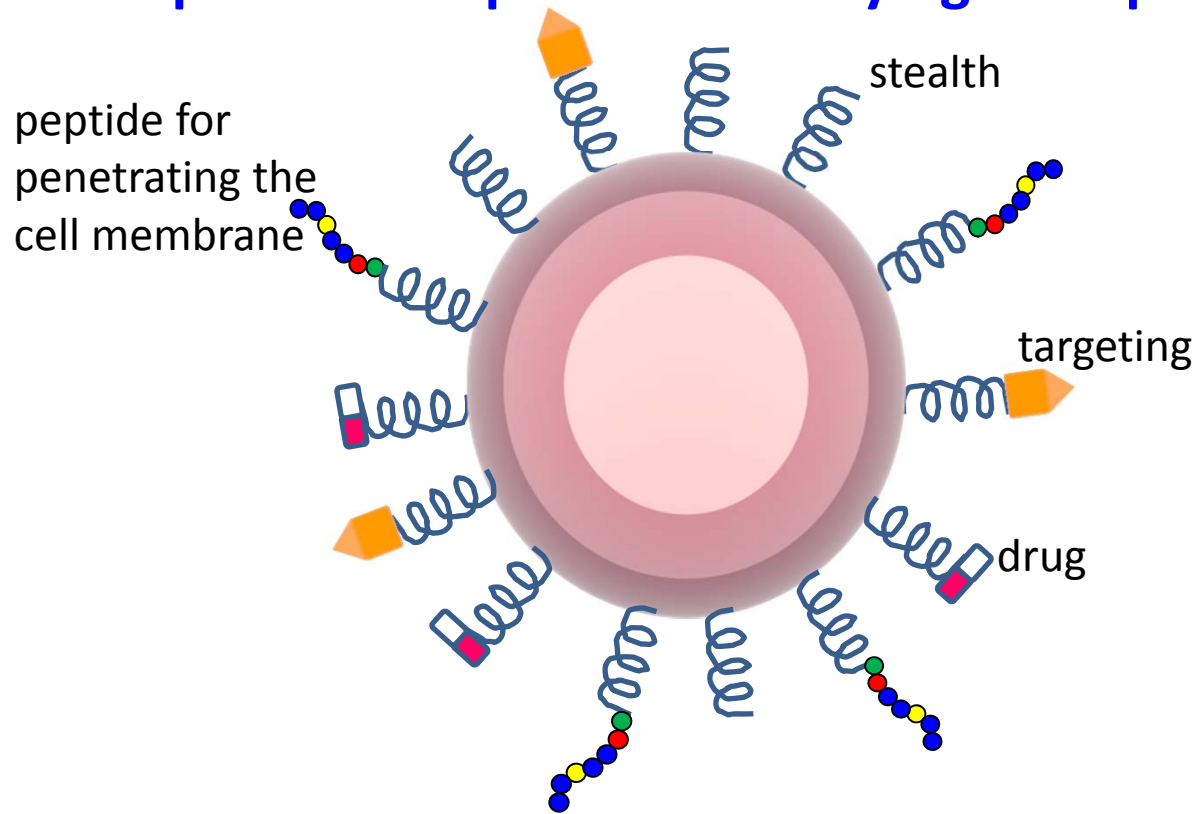


Heavy-ion accelerators for **hadrontherapy**. Available only in few clinical centers.

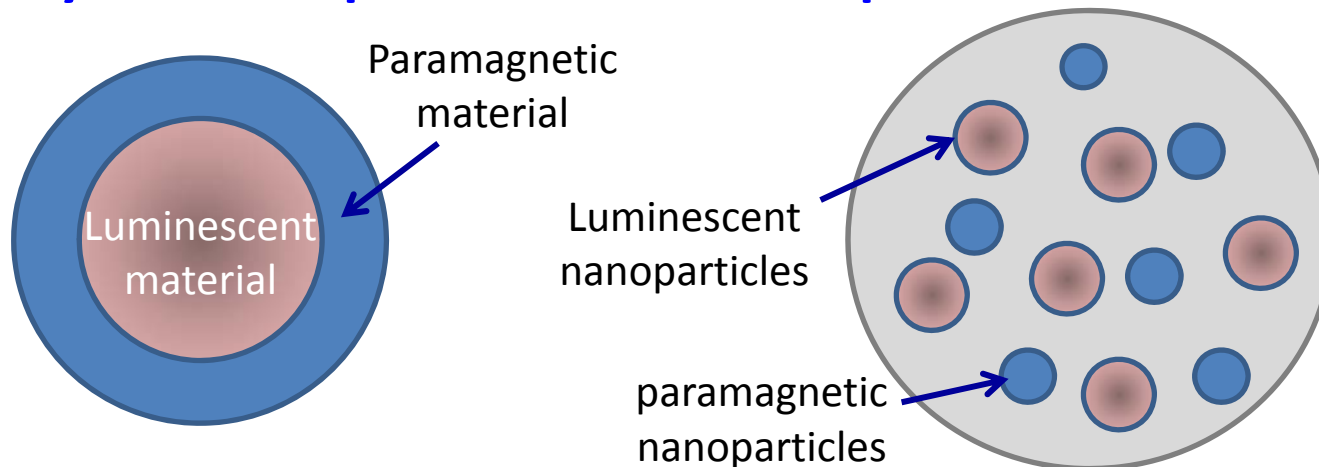
Enhanced effects with Pt NPs:
Enhanced e- emission
Higher water radical production
Higher double-strand breaks

Compare radiobiological effects by using the absorbed dose
1 Grey = 1 J absorbed per kg of matter

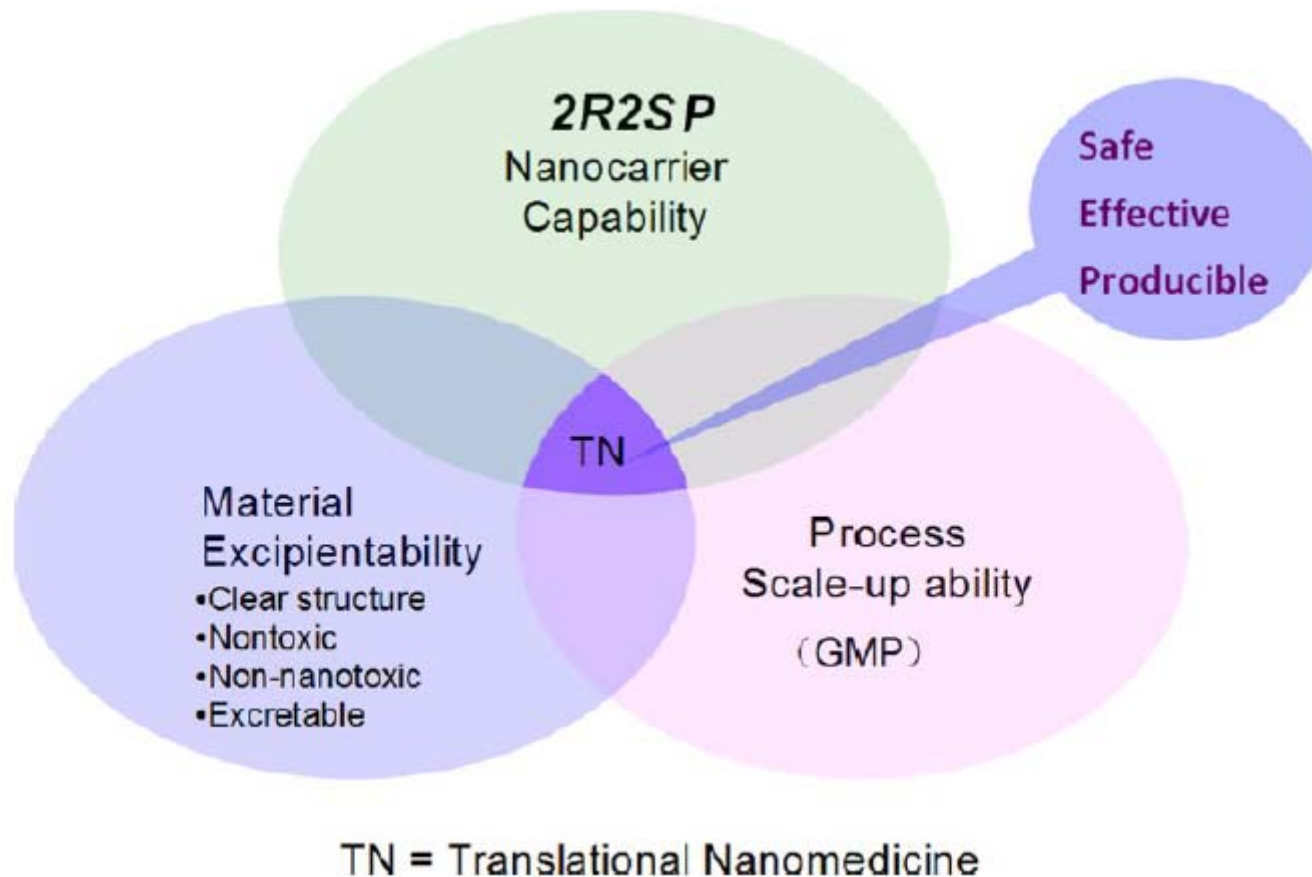
Nanoparticles as platforms carrying multiple functionalities



Hybrid nanoparticles with multiple functionalities



Translational nanomedicine



B. Pelaz, ..., W. J. Parak, ACS Nano 2017, Diverse Applications of Nanomedicine,

ACS Nano 2017, 11, 2313–2381

Regenerative medicine

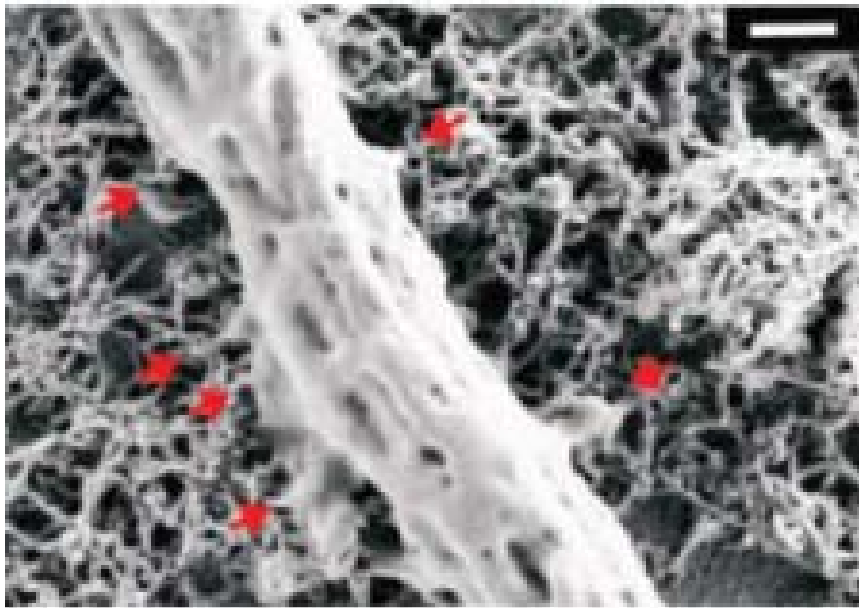
Nanoengineered implants: Polymeric scaffolds +

- NPs to tailor mechanical rigidity**
- Magnetic-NP loaded cells to control cell location and migration with external magnets**

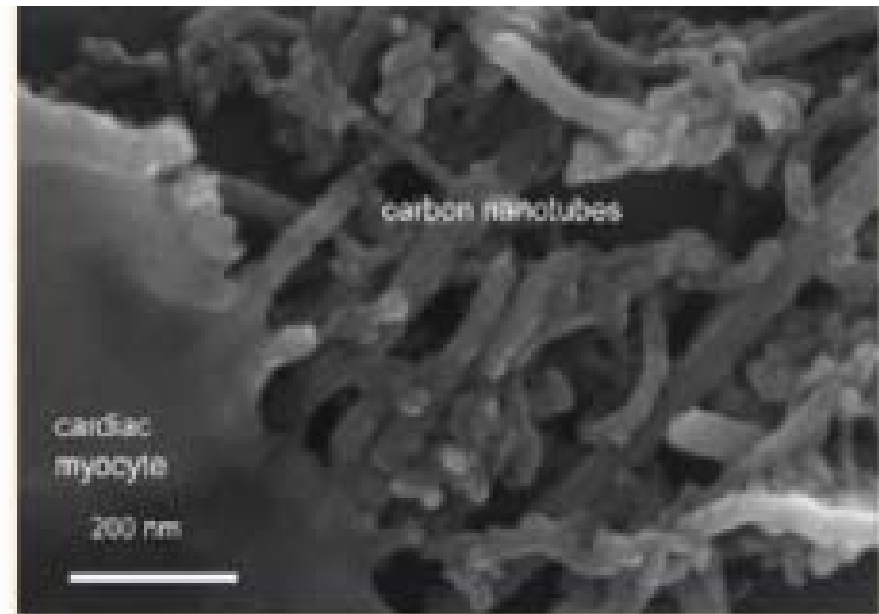
3D polymer scaffolds for

- Cell growth**
- Stem cell differentiation**

Neurons and cardiomyocytes growing on MWCNT networks



Huang, Y.-C.; Hsu, S.-H.; Kuo, W.-C.; Chang-Chien, C.-L.; Cheng, H.; Huang, Y.-Y. Effects of Laminin-Coated Carbon Nanotube/ Chitosan Fibers on Guided Neurite Growth. *J. Biomed. Mater. Res., Part A* 2011, 99A, 86–93.



Martinelli, V.; Cellot, G.; Toma, F. M.; Long, C. S.; Caldwell, J. H.; Zentilin, L.; Giacca, M.; Turco, A.; Prato, M.; Ballerini, L.; Mestroni, L. Carbon Nanotubes Instruct Physiological Growth and Functionally Mature Syncytia: Nongenetic Engineering of Cardiac Myocytes. *ACS Nano* 2013, 7, 5746–5756.